Contents lists available at SciOpen

Food Science and Human Wellness

journal homepage: https://www.sciopen.com/journal/2097-0765

Dioscin from *Polygonatum sibiricum* induces apoptosis and autophagy in Ishikawa human endometrial cancer cell and *in vivo*

Xiaoli Li[a,b,c], Runhui Ma[a,b], Zhijing Ni[a], Wei Wang[a], Kiran Thakur[a,b], Jianguo Zhang[a,b,*], Zhaojun Wei[a,b,*]

[a] *School of Biological Science and Engineering, North Minzu University, Yinchuan 750021, China*
[b] *School of Food and Biological Engineering, Hefei University of Technology, Hefei 230009, China*
[c] *School of Public Health, Anhui University of Science and Technology, Huainan 232001, China*

ARTICLE INFO

Article history:
Received 1 January 2023
Received in revised form 15 January 2023
Accepted 23 February 2023

Keywords:
Dioscin
Ishikawa cell
Apoptosis
Autophagy
PI3K/AKT
p53

ABSTRACT

With an aim to comprehend the precise regulatory mechanism of dioscin against endometrial carcinoma (EC), we firstly extracted the components from *Polygonatum sibiricum* followed by identification and structural characterization. The anti-EC activity of dioscin was initially determined based on the inhibition of Ishikawa cell proliferation and tumor growth. The high-throughput sequencing data indicated that dioscin not only promoted apoptosis, including decrease of poly ADP-ribose polymerase (PARP) and B-cell lymphoma-2 (Bcl-2) and increase of c-PARP and Bcl-2-associcated agonist of cell death (Bad), but also induced autophagy, including increase of autophagic lysosomes and LC3II/LC3I ratio. Mechanistic exploration suggested that dioscin induced autophagy and apoptosis through inhibition of PI3K/AKT/mTOR signaling pathway. Besides, the dioscin-regulated p53 pathway was mainly involved in autophagy induction. Furthermore, inhibition of Ishikawa cell autophagy was linked to dioscin-induced apoptosis. Our data suggest the immense potential of dioscin for the development of functional food for EC and related medical application.

© 2024 Beijing Academy of Food Sciences. Publishing services by Tsinghua University Press.
This is an open access article under the CC BY-NC-ND license
(http://creativecommons.org/licenses/by-nc-nd/4.0/).

1. Introduction

In countries with a very high human development index, endometrial carcinoma (EC), as reproductive tract malignant tumor of female, continues to increase with an annual incidence rate of about 1%, which is much higher than breast cancer (0.5%)[1]. According to the latest statistics of 2021, the United States alone reported 66 570 new cases and 12 940 deaths of EC[2]. In spite of the continuous progress in medical care advancements, the past two decade data reflect the acceleration of the death rates from 0.3% per year from 1997 through 2008 to 1.9% per year from 2008 through 2018, which is twice the pace of the increase in incidence[3]. The more alarming situation arises where the EC incidences are not only reported in postmenopausal women, but there are reports of its dramatical increase in younger women as well[4].

For early-stage disease, the current practice is to perform radiation and/or chemotherapy after surgery. Due to the unavailability of cure for advanced stage of the disease, chemotherapy is seen as the mainstay of treatment for most the EC patients. Due to the high tolerability and toxic side effects of traditional antineoplastic drugs, only few trials have investigated the use of chemotherapeutic agents in settings usually classified as high- or intermediate-risk disease[5]. In this scenario, the studies on natural compound therapies with exact targeted strategies along with low side effects open up new avenues for novel drug development for EC patients.

Among the important medicinal foods in China, the fleshy rhizome of *Polygonatum sibiricum* (PS) has been intensively characterized as a medicinal and nutritional supplement, and the biochemical constituents (polysaccharides, saponins, homoisoflavanones and agglutinates) of PS have been endowed with

* Corresponding authors at: School of Biological Science and Engineering, North Minzu University, Yinchuan 750021, China.
E-mail address: zhangjianguo@hfut.edu.cn (J.G. Zhang); zjwei@hfut.edu.cn (Z.J. Wei)
Peer review under responsibility of Tsinghua University Press.

SciOpen Publishing services by Tsinghua University Press

http://doi.org/10.26599/FSHW.2022.9250209
2213-4530/© 2024 Beijing Academy of Food Sciences. Publishing services by Tsinghua University Press. This is an open access article under the CC BY-NC-ND license (http://creativecommons.org/licenses/by-nc-nd/4.0/).

various health effects such as antioxidant[6], anti-tumor[7], anti-aging[8], and immune regulation[9]. The use of *Polygonatum* genus in traditional medicine has relevance to female reproductive disorders[10-11] as well as to cancer[12]. Xu et al.[13] extracted two saponin components from PS, including dioscin (diosgenyl 2,4-di-*O*-*α*-*L*-rhamnopyranosyl-*β*-*D*-glucopyranoside). While several studies have extensively shown that dioscin has an effect on inhibiting the proliferation of various human cancer cell lines[14-15]. In addition, dioscin has been reported as a potential therapeutic agent for postmenopausal osteoporosis, promising to avoid the side effects associated with hormone replacement therapy including increased risk of endometrial and breast cancer[16]. Our previous study showed that dioscin had potential health benefits in inducing cell cycle arrest and apoptosis[17]. The recent data pointed out that the increased risk of developing EC was more strongly associated with a variety of factors, including estrogen, obesity, diabetes, high blood pressure, and reproduction[18]. This indicate that the clinical efficacy of chemotherapeutic approaches for EC was of variable performance, suggesting that novel molecular therapies targeting specific cellular processes related to cell death, treatment sensitivity and drug resistance, such as autophagy, can be targeted to improve the efficacy of EC treatments. Dioscin was found to activate autophagy in hippocampal neuronal HT22 cells to prevent neurotoxicity[19]. Also, dioscin has been shown to promote autophagy in alveolar macrophages to reduce lung inflammation[20]. Furthermore, dioscin could induce autophagy in ulcerative colitis mice[21].

The complex crosstalk, interaction, and regulation of the two programmed cell death pathways, autophagy and apoptosis, on the survival or death of malignant cells have brought breakthroughs in the treatment of various tumors and other diseases. As a degradation pathway to eliminate abnormal proteins or damaged organelles in cells, autophagy is activated in response to cellular stressors. It has been revealed that regulation of both intracellular nutritional status and metabolic function (damaged proteasomes, unfolded proteins, protein aggregation and damaged organelles) can regulate the autophagy levels. At the same time, endoplasmic reticulum (ER) and mitochondrial dysfunction, DNA damage, and oxidative stress caused by external stress or stimuli can lead to the efficient induction of autophagy[22]. Nevertheless, emerging evidences have demonstrated that autophagy, triggered by the regulation of multiple signaling pathways, is involved in tumor suppression in EC[23-24]. However, it remains elusive whether dioscin can affect EC cells by activating this process.

Accumulating evidence suggested that aberrant expression of miRNAs had critical effect on the treatment resistance of numerous malignant tumors[25-27]. The positive response of miRNA-mediated gene expression regulated by natural compounds or phytochemicals in tumor therapy represents a potential molecular target in therapeutic clinical approaches. However, elucidating the effects and regulatory mechanisms of dioscin on EC from the perspective of miRNA omics has not been studied so far. Herein, based on miRNA omics data, we explored dioscin-regulated apoptosis and autophagy induction in Ishikawa cells through dynamic interactions among different signaling pathways. Further we also screened the functional miRNAs and their target genes to aim these pathways for novel therapeutic strategies.

2. Materials and methods

2.1 Chemicals

The stock solution of dioscin was prepared by dissolving in 50 mmol/L dimethyl sulfoxide (DMSO) (Lousis, MO, USA) followed by storage at −20 °C until use.

2.2 Preparation of dioscin

Dioscin was obtained from the ethanolic extract of the rhizome of PS (Qingyang, China). Firstly, the PS powder (washing, drying, crushing, and sieving) was subjected to ultrasonic (60 °C, 75 min) assisted ethanol (80%) extraction. A crude sample solution was prepared by dissolving the light brown solid obtained after evaporation under reduced pressure to no *n*-butanol[28]. Silica gel columns and Sephadex LH-20 columns were used to purify the crude product. While passing through a silica gel column, chloroform-methanol-*n*-butanol-water (10:5:1:4, *V*:*V*) was used the eluent, and when passing through a Sephadex LH-20 column, ethanol-water gradient was used as the eluent. HPLC (Thermo Fisher, USA) was used for purity analysis. Ultra performance liquid chromatography-time of flight-tandem mass spectrometry (UPLC-TOF-MS/MS) (Waters Corporation, Milford, MA, USA) was used to perform molecular weight analytical determinations in positive ion detection mode. VNMRS600 Nuclear magnetic resonance (NMR) spectrometer (Agilent, USA) was used for molecular structure determination.

2.3 Cell culture

According to our previously reported method[17], human EC cell line, Ishikawa and human embryonic kidney cells (HEK293) were cultured after procurement from Wuhan Procell Life Technology Co., Ltd. (China).

2.4 Cell viability assays

For this, cells (8×10^3 cells/well in 96-well) were seeded overnight followed by treatment with several concentrations of dioscin (0, 1, 2, and 3 μmol/L) for 24 h. According to the manufacturer's procedure, 10 μL of CCK-8 reagent (Beyotime, Shanghai, China) was added to each well and cells were further allowed to incubate for 2 h. The cell growth was assessed in terms of the absorbance ($A_{450\ nm}$) using a microplate reader (Bio-Rad Laboratories Ltd., China)[29].

2.5 Tumor xenograft models

According our previous study[30], specific mice model was obtained by subcutaneously injecting the Ishikawa cells (1×10^7 cells/mL) under specific pathogen-free conditions. The mice were randomly divided into dioscin group (24 mg/kg)[31-33] and control group (treated with equal volume of DMSO) (Con group). Mice body weight and tumor volume were monitored every other day over a 21-day period of i.p. dosing. Finally, the treated mice were sacrificed at the end of the treatment, and 4 micron-thick serial sections of xenograft organs and tumor tissues were used for terminal deoxynucleotidyl

transferase-mediated dUTP-biotin nick end labeling (TUNEL) and hematoxylin-eosin (H&E) staining.

2.6 RNA extraction, library construction, and sequencing

The dioscin (2 μmol/L) treated and the control groups were set for 3 biological replicates. After the total RNA isolation using TRIzol reagent (Invitrogen, CA, USA), its auality and quantity were assessed using a 2100 Bioanalyzer (Agilent Technologies, Santa Clara, CA, USA). For RNA-Seq (Hangzhou Lianchuan Biotech (LC-Bio) Technology Co., Ltd., library construction procedures were performed by standard Illumina sample preparation protocols. The mRNA sequencing was outsourced using the Illumina Novaseq™ 6000 platform[30].

2.7 Analysis of DEMs and DEGs

The differential expression of mRNA and miRNA between the dioscin group and the Con group was analyzed using DESeq2 package in the statistics software. Differentially expressed miRNAs (DEMs) were identified to setup the fold change ($|\log_2 FC| > 1$ and q value (adjusted P-value) < 0.05. The genes with $|\log_2 FC| > 1$ and $P < 0.01$ were regarded as differentially expressed genes (DEGs). These results were visualized using volcano plots and principal component analysis (PCA) built by the R language[34].

2.8 Function enrichment analysis and miRNA-mRNA regulatory network analysis

The targets of miRNAs were predicted using Targetscanb and miRanda softwares. A Gene Ontology (GO) enrichment analysis was performed on target genes with GOseq R package. All the target genes were also subjected to Kyoto Encyclopedia of Genes and Genomes (KEGG) enrichment analysis. Cytoscape software was used to screen out core regulatory genes based on the protein-protein interaction (PPI) network and visualize the interaction network between miRNA and mRNA[35].

2.9 Transmission electron microscopy analysis

Based on our previous study, dioscin treated ishikawa cells (2 μmol/L) and control group were harvested followed by 4 h of fixation (2.5% glutaraldehyde) at 4 °C, phosphate buffered saline (PBS) rinsing, and then further 2 h of fixation (1% osmium tetroxide). The after, the dehydration of samples was performed in a gradient of ethanol solutions followed by embedding in Araldite 812. The selected areas were cut using the Leica UC7 ultramicrotome with a diamond slicing knife. Ultrathin sections (60−80 nm) were stained with 2% uranyl acetate saturated alcohol solution and 2% lead citrate. Subsequently, the samples were observed under transmission electron microscope (TEM) system (HT7700, Hitachi, Japan)[36].

2.10 Immunohistochemistry and immunofluorescence assays

Tumor sections were prepared following the standard protocols. Sections were incubated with antibodies against caspase 9 (1:100, *VIV*), p-AKT (1:200), Beclin-1 (1:2 500) and p-p53 (1:200) overnight, followed by the addition of secondary antibodies and incubation for 0.5 h. Diaminobenzidine was used for the color reaction[37].

For immunofluorescence, following steps were involved: PBS washing of the treated cells, 4% paraformaldehyde fixation, 0.1% Triton X-100 permeabilization, and 0.1% bovine serum albumin (BSA) blocking. After the above steps, cells were incubated with anti-LC3B (1:200, *VIV*), secondary antibody, and 4′,6-diamidino-2-phenylindole (DAPI) overnight (4 °C) and for 1 h (room temperature), and for 30 min, respectively. Lastly, the cells were examined and analyzed under a fluorescence microscope (Olympus, X51, Japan) and Image Pro Plus (version 6.0, Media Cybernetics Inc., Rockville, MD, USA), respectively[38].

2.11 Western blotting analysis

Total proteins from Ishikawa cells and tumor tissues were extracted using lysate containing protease inhibitors, and quantified using BCA protein assay reagent (Thermo Scientific, USA). The total protein (same amount) from each sample was separated by 10% sodium dodecyl sulfate-polyacrylamide gel electrophoresis (SDS-PAGE) and then electro transferred to polyvinylidene fluoride (PVDF) membranes (Millipore Darmstadt, Germany) for immunoblotting. After blocking, the membranes were incubated with 1° and 2° antibodies overnight at 4 °C and for 1 h at room temperature, respectively. Protein band detection was accomplished with enhanced chemiluminescent Western blotting reagents and protein expression was calculated using ImageJ software[39].

2.12 Validation of mRNA and miRNA expression by qRT-PCR

The mRNA and miRNA expression were verified using real time quantitative polymerase chain reaction (RT-qPCR) analysis and primers used were listed in the Tables 1 and 2. The cDNA was synthesized by Evo M-MLV RT Mix Kit (AGbio, Hunan, China), according to the manufacturer's protocol. For mRNA and miRNA quantitative PCR analysis, SYBR Green Premix Pro *Taq* HS qPCR Kit (AGbio, Hunan, China) and miRNA fluorescent quantitative PCR (dye method) kit (Sangon Biotech, Shanghai, China) were used on Real-Time PCR System (LightCycler® 480 SYBR Green I Master)[24].

Table 1
microRNA primers for qRT-PCR.

miRNA	Sequence (5′-3′)
mir-1246-p5_1ss17AG	GGATTTTTGGAGCAGGGAG
mir-2887-1-p5	GACCGGGGTCCGGTGCGGA
mir-6236-p3_1	AATGGATGGCGCTGGAGC
miR-19b-3p	TGTGCAAATCCATGCAAAACTGA
miRNA-1260	ATCCCACCGCTGCCACCA
miR-1180-5p_R-1	GGACCCACCCGGCCGGGAAT
miR-1287-5p	TGCTGGATCAGTGGTTCGAGTC
miR-10395-3p	ATGTATTCGTACTGTCTGATG

Table 2
Gene primers for qRT-PCR.

Gene	Forward primer (5′-3′)	Reverse primer (5′-3′)
NGF	GGCAGACCCGCAACATTACT	CACCACCGACCTCGAAGTC
LAMA3	CACCGGGATATTTCGGGAATC	AGCTGTCGCAATCATCACATT
FGF2	AGAAGAGCGACCCTCACATCA	CGGTTAGCACACACTCCTTTG
IL4R	CGTGGTCAGTGCGGATAACTA	TGGTGTGAACTGTCAGGTTTC
GADD45A	CCCTGATCCAGGCGTTTTG	GATCCATGTAGCGACTTTCCC
TP53AIP1	CGGGGAATAGAAGCTCTGTCA	CTGGAGAGACCTAGACCAAGG
PRLR	TCTCCACCTACCCTGATTGAC	CGAACCTGGACAAGGTATTTCTG
LPAR3	GCTGCCGATTTCTTCGCTG	AGCAGTCAAGCTACTGTCCAG
β-actin	TGTCACCAACTGGGACGATA	GGGGTGTTGAAGGTCTCAAA

2.13 Statistical analysis

Results (mean ± SD) were processed for statistical significance using one-way analysis of variance (ANOVA) in SPSS software version 19.0 (SPSS Inc., Chicago, IL, USA) at $P < 0.05$.

3. Results

3.1 Dioscin extraction from PS

The extracted compound was reported with 97.14% as the main peak situated at 2.86 min (Fig. 1A). And $[M + H]^+$ peak at *m/z* 869.488 0, $[M – Rha + H]^+$ peak at *m/z* 723.430 2, $[M – 2Rha + H]^+$ peak at *m/z* 573.372 7, and $[M – 2Rha – Glc + H]^+$ peak at *m/z* 415.320 0 revealed the molecular weight of the compound as 869.04 Da (Fig. 1B), which corresponded to the earlier reports[14,40]. According to the NMR data, the obtained compound was identified as dioscin (Figs. 1C-E). ^{13}C NMR (151 MHz, DMSO) δ: 152.34, 140.72, 121.69, 108.84, 100.94, 100.74, 98.61, 88.01, 80.62, 77.39, 77.05, 76.68, 76.56, 75.67, 72.34, 71.16, 71.04, 71.01, 70.87, 69.08, 68.39, 66.35, 62.23, 60.43, 56.21, 50.00, 41.53, 40.34, 40.22, 40.20, 40.06, 39.92, 39.78, 39.64, 39.55, 39.50, 38.03, 37.25, 36.83, 31.96, 31.92, 31.41, 31.38, 30.25, 29.46, 28.91, 20.82, 19.40, 18.25, 18.20, 17.53, 16.46, 15.11. ^{1}H NMR (600 MHz, DMSO-d6) δ: 5.30 (d, J = 5.0 Hz, 1H), 5.00 (d, J = 1.6 Hz, 1H), 4.72–4.62 (m, 5H), 4.57 (d, J = 4.3 Hz, 1H), 4.46 (dd, J = 15.6, 5.8 Hz, 2H), 4.37 (d, J = 7.9 Hz, 1H), 4.25 (q, J = 7.3 Hz, 1H), 3.96 (dt, J = 9.3, 6.1 Hz, 1H), 3.83 (dq, J = 9.4, 6.2 Hz, 1H), 3.60–3.53 (m, 2H), 3.48–3.34 (m, 6H), 3.23–3.14 (m, 3H), 3.15 (s, 2H), 2.41–2.35 (m, 1H), 2.17–2.10 (m, 1H), 1.89 (ddd, J = 19.0, 15.1, 10.1 Hz, 2H), 1.77 (qd, J = 12.3, 11.0, 5.7 Hz, 3H), 1.69–1.62 (m, 2H), 1.62–1.48 (m, 4H), 1.49–1.38 (m, 4H), 1.14 (ddd, J = 24.4, 12.9, 5.1 Hz, 2H), 1.07 (dd, J = 9.4, 6.1 Hz, 7H), 0.96 (dd, J = 13.7, 4.2 Hz, 1H), 0.93 (s, 3H), 0.88 (d, J = 6.9 Hz, 4H), 0.71 (t, J = 3.2 Hz, 6H).

3.2 Dioscin decreased Ishikawa cell viability

The viability of dioscin treated EC Ishikawa cell was reduced in a concentration-dependent manner (Fig. 2A). In contrast, the effect of dioscin on the cell viability of the normal cell line (HEK293) was higher than 80% at the concentration of 0−4 μmol/L (Fig. 2B). Based on the comparative results in Fig. 2C, we selected 2 μmol/L dioscin treatment on Ishikawa cells as the most suitable concentration for subsequent experiments. These results indicated that dioscin was a natural compound with better anti-cancer effects.

3.3 Dioscin inhibited tumor growth

Our *in vivo* results (effects of dioscin on tumor growth) showed that tumor size was suppressed after treatment with dioscin (Figs. 3A-B). A noteworthy decrease in tumor volume (Fig. 3D) and weight (Fig. 3E) was confirmed after treatment with dioscin (24 mg/kg) in comparison to the control group ($P < 0.05$). Fig. 3C revealed the upward trend in the body weight of mice but without any significant difference between the treated and control groups. In addition,

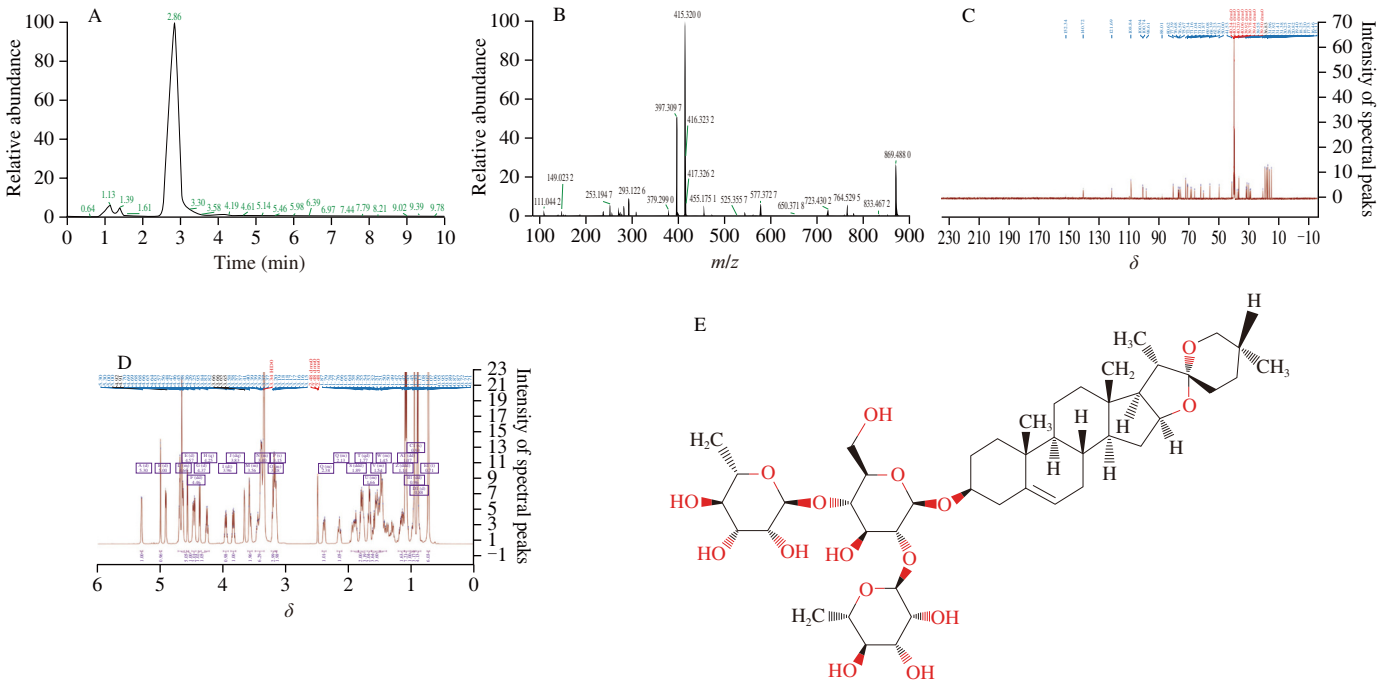


Fig. 1 HPLC chromatograms (A), MS spectrum (B), ^{13}C NMR spectra (C), ^{1}H NMR spectra (D) and structure (E) of dioscin.

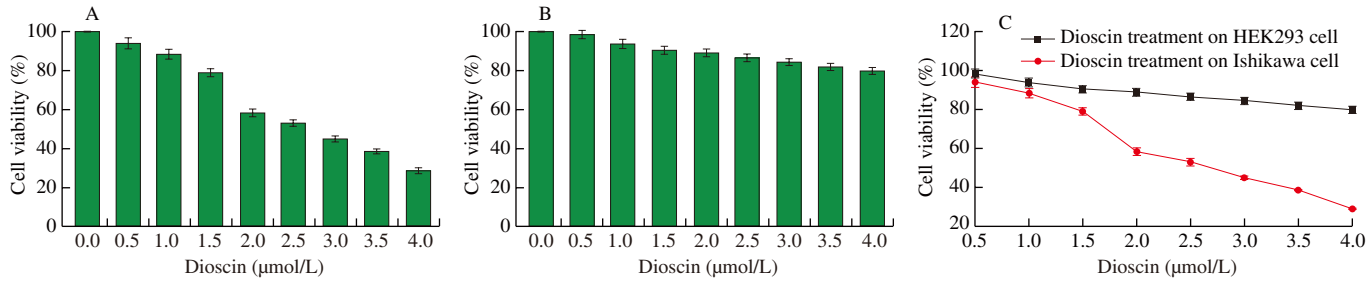


Fig. 2 Viability of dioscin on Ishikawa cell (A) and HEK293 cell (B) at 24 h. (C) Comparison of dioscin treatment on the cell viability of HEK293 and Ishikawa cell at 24 h. The data were presented as means ± SD of triplicates experiments.

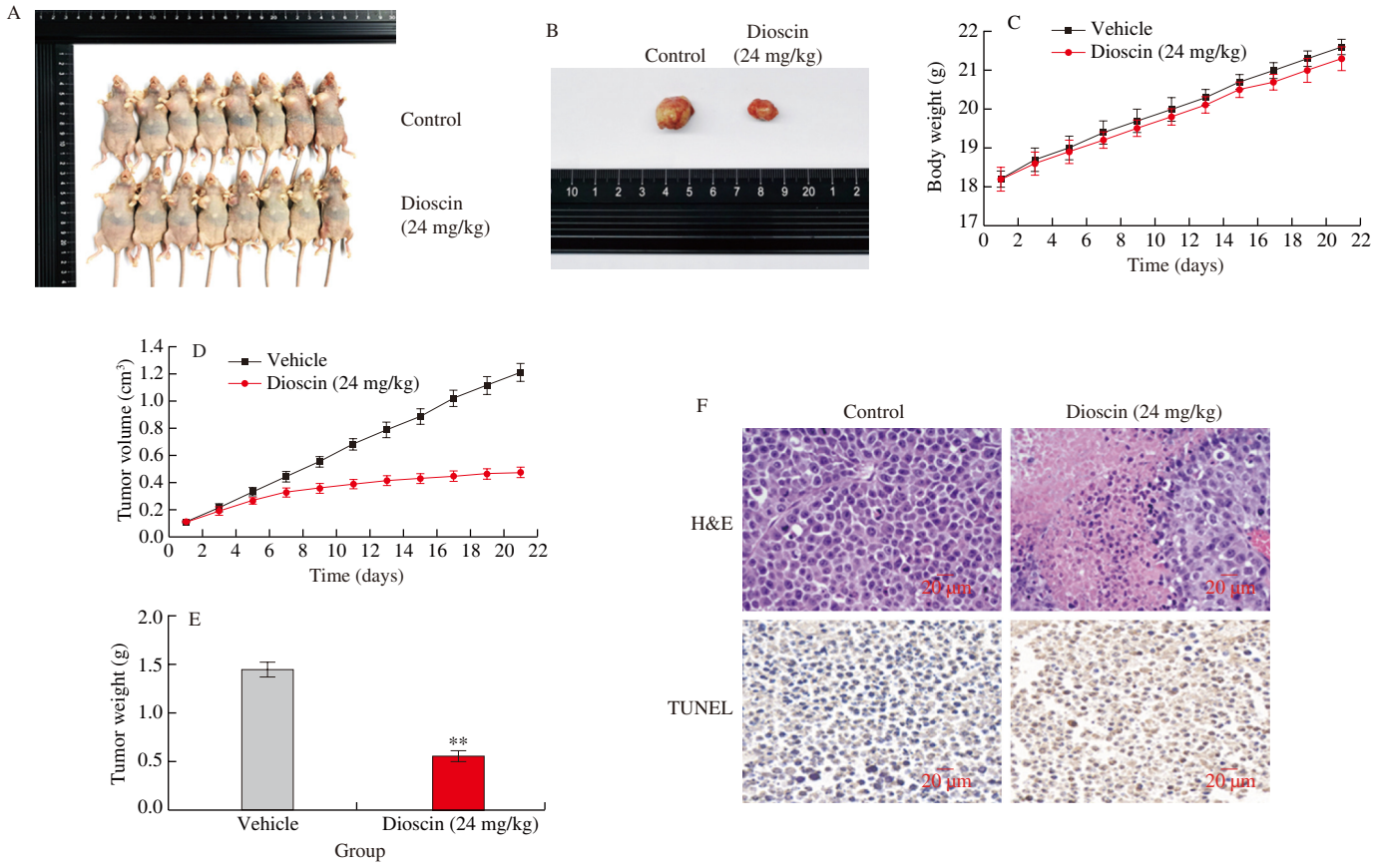


Fig. 3 Dioscin (24 mg/kg) suppressed tumor growth in xenograft model. (A-B) Comparison of control and dioscin group for xenograft sacrificed of mice and tumour size. Body weights (C), tumor volume (D), and tumor weights (E) of xenograft mice in control group and dioscin treatment group. (F) Image of immunohistochemical staining for H&E staining and TUNEL staining in tumor tissues between control group and dioscin group. All the data were presented as the mean ± SD. *$P < 0.05$ and **$P < 0.01$ versus control group.

histological analysis was utilized to detect apoptosis of tumor cells *in vivo* (Fig. 3F). The dioscin treated tumor tissues exhibited significant tissue disorders and larger necrotic areas. More tunel-positive cells were found in xenografts treated with dioscin in comparison to the control group. These results further established the inhibitory effect of dioscin on endometrial tumor growth *in vivo* and indicated the association with the apoptosis induction in Ishikawa cells.

3.4 *Identification of differential expressed miRNAs*

The PCA in Fig. 4A more clearly showed the within-sample similarity and between-sample variability. The volcano plot (Fig. 4B) and heat map (Fig. 4C) directly reflected those 62 miRNAs which had significant changes ($P < 0.05$) in the treatment group, with 25 miRNAs increasing and 37 miRNAs decreasing trend. Table 3 presented the DEMs after dioscin treatment.

3.5 *Function enrichment analysis of DEMs target genes*

The target genes of DEMs were predicted using TargetScan and miRanda software, and further functional enrichment analysis was performed. Fig. 4D revealed the target genes of DEMs mainly involved in the signal transduction process ontology of biological process ontology, protein blindness of molecular function and cell membrane of cellular components. Notably the KEGG enrichment results showed that the target genes of DEMs were mainly enriched

in PI3K/AKT, p53, and autophagy signaling pathways. This aroused our keen interest to continue to unravel thev possible regulatory mechanisms of dioscin on Ishikawa cells to inhibit EC progression.

Table 3
Total DEMs in dioscin group compared with the control group.

miRNAs	*P* value	$\log_2$ FC	Expression
Upregulated miRNA			
miR-2904-2-p5	2.49×10^{-3}	1.99	High
miR-1246-p5_1ss17AG	2.95×10^{-3}	2.42	Low
miR-2887-1-p5	3.39×10^{-3}	2.27	Middle
miR-2887-1-p5_1ss21AT	7.65×10^{-3}	2.11	Middle
miR-2887-1-p3_1ss11AT_1	1.13×10^{-2}	1.38	High
miR-2887-1-p3_1ss11AT_2	1.13×10^{-2}	1.38	High
miR-6236-p5_4	1.59×10^{-2}	1.91	High
miR-6236-p5_1	1.59×10^{-2}	1.91	High
miR-6236-p3_4	1.59×10^{-2}	1.91	High
miR-6236-p5_2	1.59×10^{-2}	1.91	High
miR-6236-p5_3	1.59×10^{-2}	1.91	High
miR-1246_L+4	1.91×10^{-2}	3.49	Low
miR-19b-3p	2.23×10^{-2}	1.19	Middle
miR-12136_R+8	2.25×10^{-2}	4.31	High
miR-6240-p3_1ss10TG_2	2.44×10^{-2}	2.18	High
miR-6240-p3_1ss10TG_1	2.44×10^{-2}	2.18	High
miR-6236-p3_1	2.45×10^{-2}	1.51	Middle
miR-6236-p3_3	2.45×10^{-2}	1.51	Middle
miR-6236-p3_2	2.45×10^{-2}	1.51	Middle
miR-27a-5p	3.21×10^{-2}	1.06	Middle
miR-1246_L-1R+3	4.07×10^{-2}	2.68	Middle
miR-1246_L+4R+1	4.35×10^{-2}	3.40	Middle
miR-1246_L+5R+1	4.42×10^{-2}	4.06	Middle
miR-2904-2-p3	4.60×10^{-2}	1.47	High
miR-1246_L+1R+2	4.85×10^{-2}	3.73	High
Downregulated miRNA			
PC-3p-45158_31	1.68×10^{-3}	−inf (negative infinity)	Low
miR-1260b_L+1_1ss10AG	4.72×10^{-3}	−inf	Low
miR-4454_L-2	7.41×10^{-3}	−2.32	Middle
miR-24-1-p5_1ss2GC	9.07×10^{-3}	−2.21	Middle
miR-429-p5	9.59×10^{-3}	−inf	Middle
miR-9995-3p_L+1_1	1.12×10^{-2}	−inf	Low
miR-9995-3p_L+1_2	1.12×10^{-2}	−inf	Low
miR-4787-3p	1.21×10^{-2}	−inf	Low
miR-8903_R-2_1ss17CT	1.48×10^{-2}	−inf	Low
miR-378d_R-2	1.54×10^{-2}	−1.44	Middle
miR-1260	1.56×10^{-2}	−1.62	High
miR-940	1.62×10^{-2}	−1.59	Middle
miR-1260b_R+1_1ss9AG	1.93×10^{-2}	−2.74	Middle
miR-3180_R+2	2.14×10^{-2}	−inf	Low
miR-1260_L+2	2.16×10^{-2}	−1.20	Middle
miR-877-3p_R+1	2.17×10^{-2}	−1.02	Middle
miR-1180-5p_R-1	2.25×10^{-2}	−2.57	Middle
miR-1260b_R-1	2.39×10^{-2}	−1.05	Middle
miR-135a-2-3p_R-1	2.40×10^{-2}	−inf	Low
miR-339_R+1_1ss21AT	2.40×10^{-2}	−inf	Low
PC-5p-57106_14	2.42×10^{-2}	−inf	Low
miR-1287-5p	2.72×10^{-2}	−2.60	Middle
miR-328-3p	3.00×10^{-2}	−1.21	Middle
miR-125b-2-3p_L-2R+2	3.05×10^{-2}	−1.04	Middle
miR-9993b-3p_1ss1AT	3.29×10^{-2}	−1.45	Middle
miR-1246_L+1R-2	3.33×10^{-2}	−1.75	Middle
miR-1273c-p3	3.65×10^{-2}	−1.98	Middle
miR-10395-3p	3.72×10^{-2}	−2.07	Middle
miR-551a-p5	3.83×10^{-2}	−inf	Low
miR-9993b-3p	3.89×10^{-2}	−1.27	Middle
miR-3944-5p	4.08×10^{-2}	−2.81	Middle
miR-1908-5p	4.24×10^{-2}	−1.47	Middle
miR-338-5p_R-1	4.45×10^{-2}	−2.31	Low
miR-9933_L-4_1ss12AT	4.48×10^{-2}	−2.36	Middle
PC-3p-41724_41	4.48×10^{-2}	−2.27	Low
miR-1260_L+1	4.61×10^{-2}	−1.51	Middle
miR-550a-5p_R-2	4.73×10^{-2}	−1.16	Middle

3.6 Dioscin prompted apoptosis and autophagy

Based on the experiments in which dioscin reduced the viability of EC cells and inhibited tumor proliferation in mice, and in conjunction with the high-throughput histological studies, the final enriched cellular pathways were found to be mainly involved in the autophagy-apoptosis interaction regulatory signaling pathways PI3K/AKT and p53, and it is reasonable to infer that dioscin is more likely to act on autophagy and apoptosis. In our previous study[17], it was confirmed that dioscin induced apoptosis through cell cycle arrest and mitochondrial pathway. Here, we further confirmed the effects of dioscin on apoptosis and autophagy in Ishikawa cells by tumor immunohistochemistry. The increase of bright blue cells in DAPI staining indicated that dioscin indeed triggered apoptosis (Fig. 5A). The enhancement of red light in LC3 staining also tentatively indicated that dioscin regulated activities related to cellular autophagy which was further confirmed by TEM assay. Comparison of the control and the treated groups revealed an increase in autophagic lysosomes in the cells in the dioscin-treated group (Fig. 5B).

The effects of dioscin on apoptosis and autophagy marker protein expression were further examined at the *in vivo* and *in vitro* translation levels. Western blot results (Figs. 6A-B) demonstrated that the protein Bcl-2 and PARP were significantly decreased, and protein Bad and c-PARP was significantly upregulated in the dioscin-treated group ($P < 0.05$). The levels of autophagy-related protein Beclin-1 and the ratio of LC3II/LC3I were significantly increased and the expression of p62 protein was decreased ($P < 0.05$). In addition, immunohistochemical analysis (Fig. 6C) also showed that treatment with dioscin reduced the level of tumor protein caspase 9 and increased the positive expression of Beclin-1. The results demonstrated the promotion of apoptosis and autophagy in Ishikawa cells under the effect of dioscin. Combining with the histological data, we next investigated the PI3K/AKT pathway and p53 signaling pathway at the *in vivo* and *in vitro* protein levels, respectively, to further explore the underlying mechanism of dioscin effects on Ishikawa apoptosis and autophagy.

3.7 Inhibition of dioscin on PI3K/AKT pathway

In the aforementioned results of this study, high-throughput sequencing and gene enrichment studies revealed a close association between the target of dioscin and the PI3K/AKT signaling pathway. The protein immunoblotting assay observed that dioscin downregulated PI3K expression in Ishikawa cells. The total protein levels of AKT and mTOR did not change significantly, while the phosphorylation levels of mTOR and AKT were significantly decreased (Fig. 7A). The same protein expression results were also shown in dioscin-treated mouse tumors (Fig. 7B). Immunohistochemical results also confirmed the diminished p-AKT protein levels *in vivo* (Fig. 7C). We next examined apoptosis and autophagy marker proteins using AKT inhibitor and AKT phosphorylation activator (SC79), respectively (Fig. 7D). We found that dioscin and inhibitor III had the same regulatory effect on p-AKT expression. Compared to the dioscin-treated group, the down-regulated phosphorylated AKT levels were found to be increased when Ishikawa cells were treated with SC79 and dioscin in culture. This suggested that dioscin was involved in regulating the PI3K/AKT pathway. And in this process, when SC79 stimulated

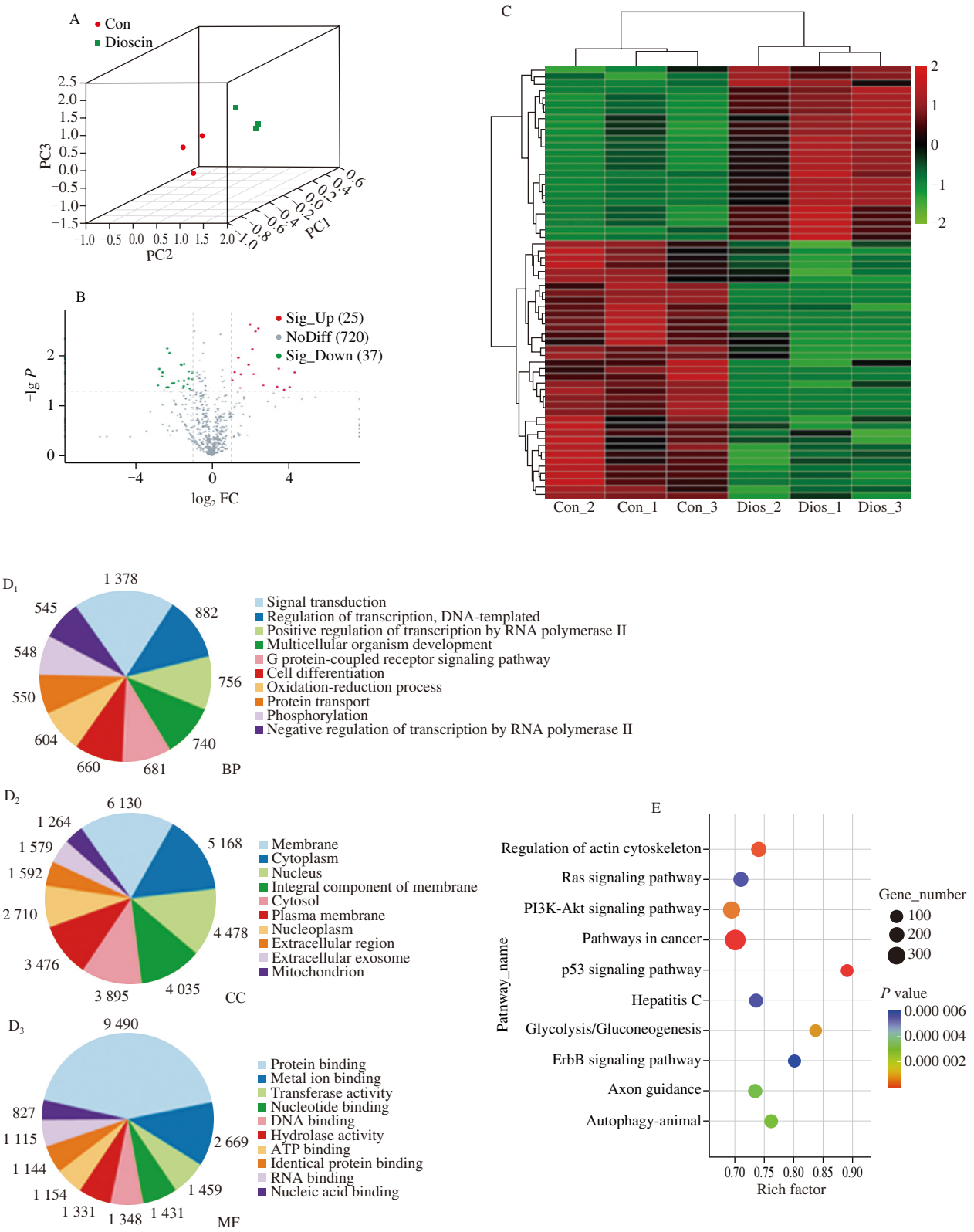


Fig. 4 miRNA-sequencing analysis of dioscin (2 μmol/L) treated Ishikawa cells. (A) PCA of all samples. (B) Volcano plot of DEMs between control and dioscin-treated samples ($P < 0.05$). (C) Heat map of DEMs. GO (D) and KEGG (E) enrichment analysis of target genes for DEMs in Ishikawa cells.

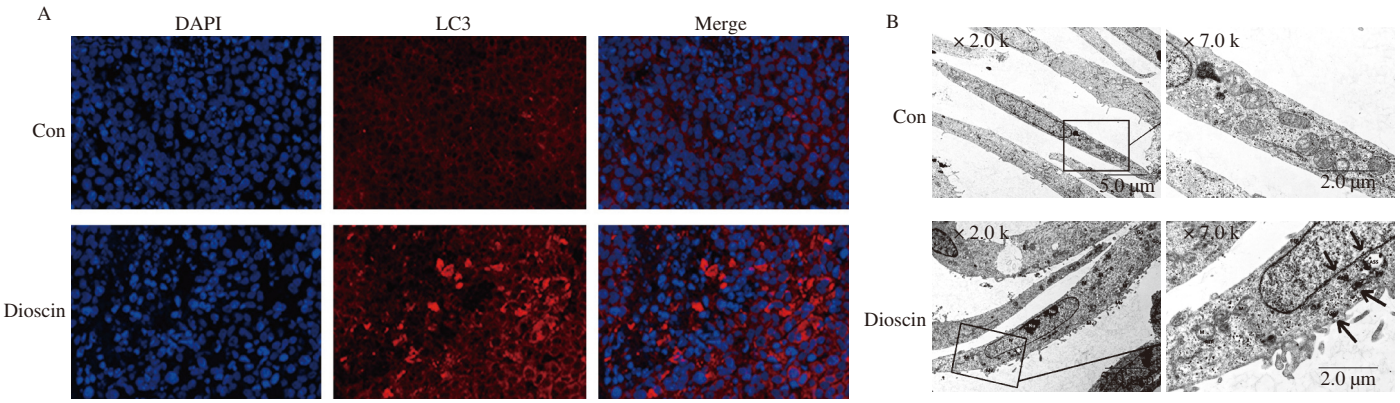


Fig. 5 Occurrence of apoptosis and autophagy in dioscin-treated Ishikawa cells. (A) Immunofluorescence images of DAPI and LC3 (400×, Scale bar = 50 μm). (B) Transmission electron microscopy images of increased autophagic autolysosomes (ASS) in dioscin-treated Ishikawa cells (ASS were indicated by black arrows).

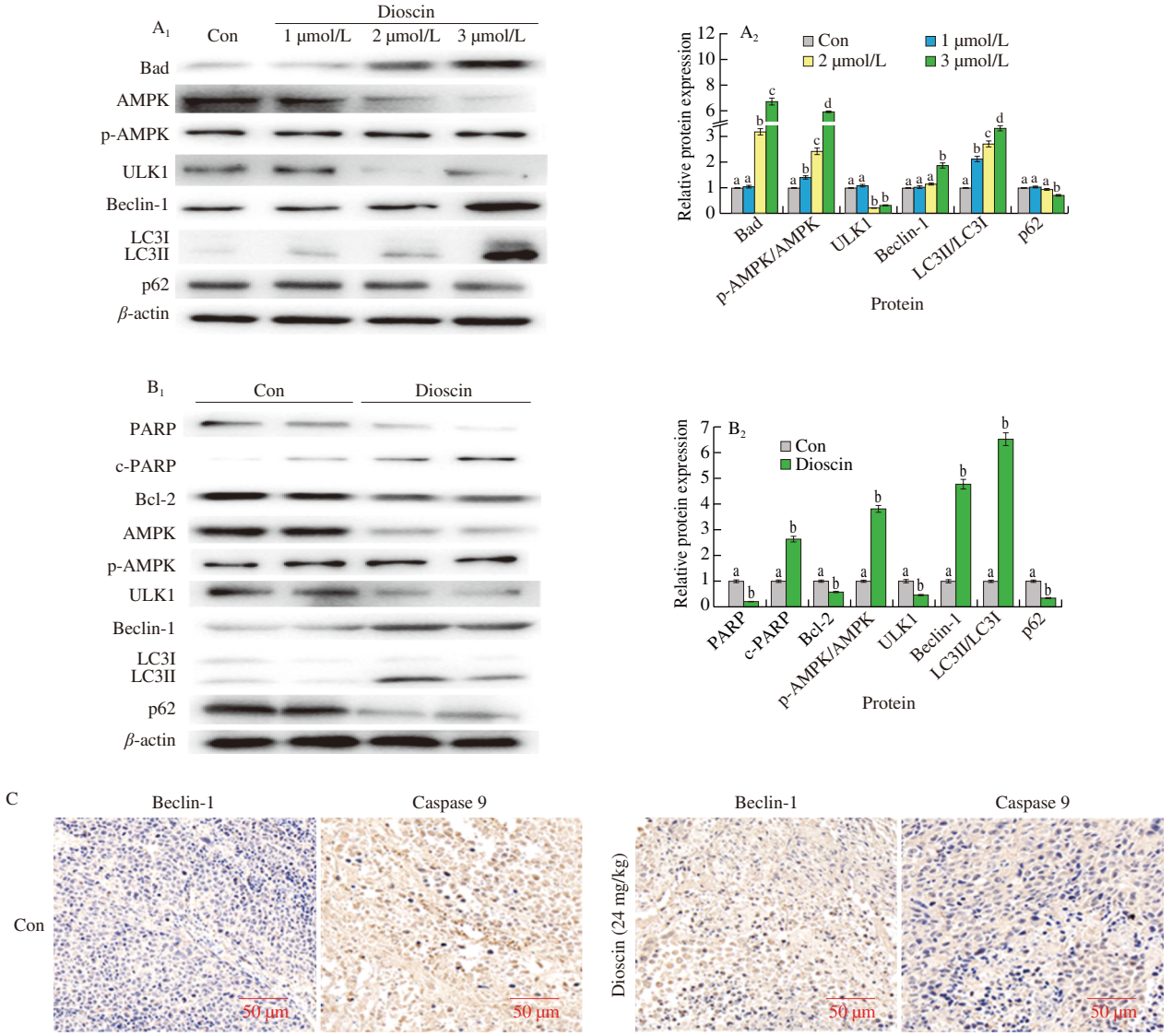


Fig. 6 Dioscin induced apoptosis and autophagy of endometrial cancer cells *in vitro* and *in vivo*. (A) Immunoblotting analysis and quantification of apoptosis and autophagy associated proteins in Ishikawa cells. (B) Protein expression profile and relative expression levels in tumor. (C) Immunohistochemistry images of Caspase 9 and Beclin-1 expression in tumor tissues. Significant differences between groups were represented by different lowercase letters ($P < 0.05$, $n > 3$). The same below.

the p-AKT level to rise, p62 rebounded and caspase 3 was activated. Besides, the addition of dioscin significantly attenuated p-ATK after SC79 treatment of Ishikawa cells in culture. At the same time, the up-regulated apoptotic protein caspase 3 and autophagy protein p62 were also decreased. This confirmed that dioscin promoted apoptosis and autophagy in Ishikawa cells by suppressing the PI3K/AKT pathway.

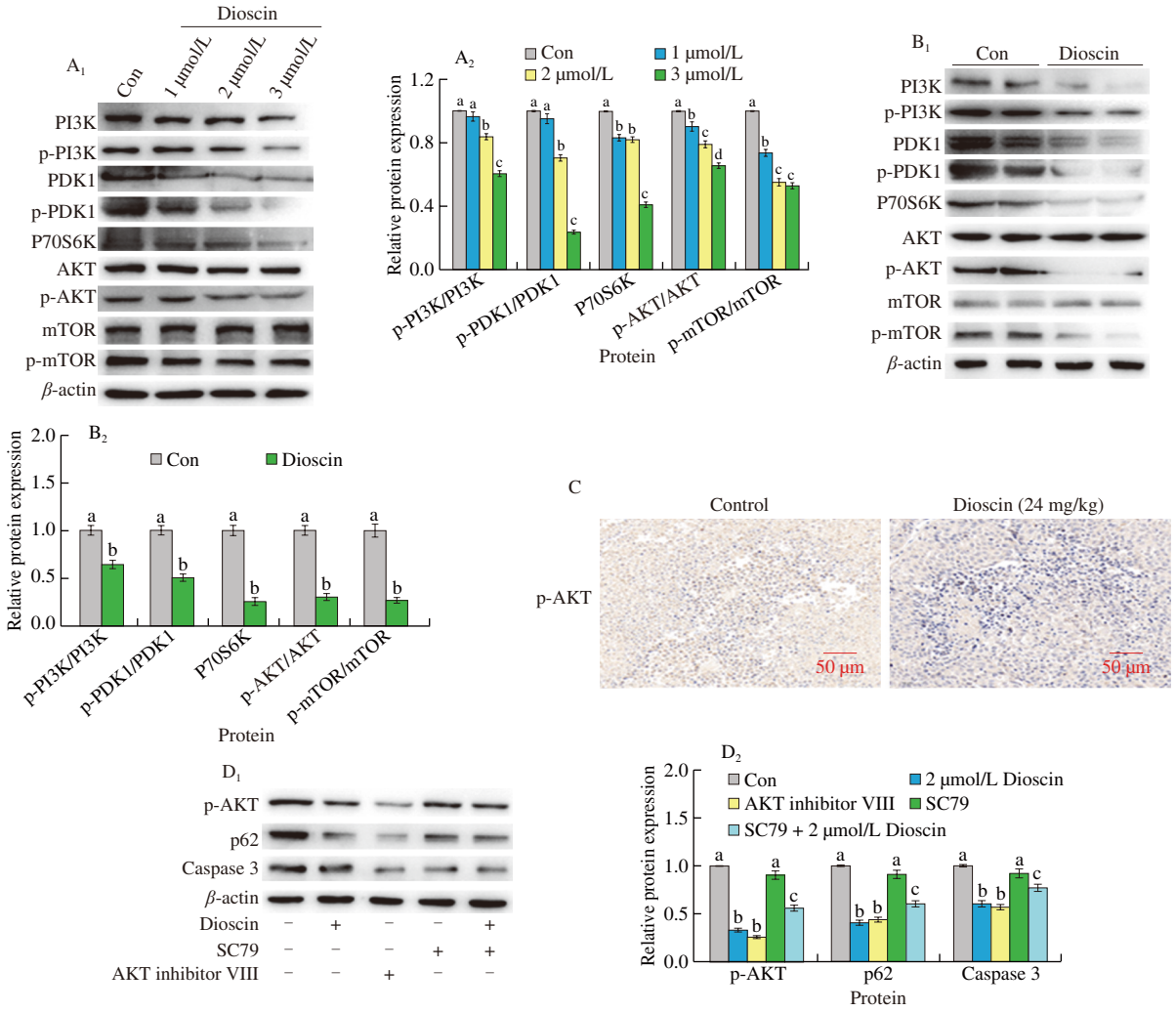


Fig. 7 Immunoblotting analysis for the protein of PI3K/AKT/mTOR signaling pathway. Protein expression profile and relative expression levels *in vitro* (A) and *in vivo* (B). (C) Immunohistochemistry for the detection of p-AKT expression in tumor sections. (D) Western blot analysis of p-AKT, Caspase 3 and p62 in Ishikawa cells after treatment of dioscin (2 μmol/L), AKT inhibitor VIII and SC79.

3.8 Activation of dioscin on p53 pathway

The p53 protein was considered a tumor suppressor that can regulate both apoptosis and autophagy. Under conditions such as DNA damage, the p53 gene was activated in cells and it could promote apoptosis by upregulating the expression of pro-apoptotic genes. Upon stimulation, p53 migrated to the nucleus and bound to the pro-expression region of the autophagy-promoting gene AMPK to increase the level of autophagy. In the KEGG enrichment analysis, the p53 signaling pathway was recognized as a high significance and enrichment factor (Fig. 4E). Thus, the potential of p53 signaling in the treatment of EC was further explored. As shown in Fig. 8A, after treatment with dioscin, cellular p53 protein expression was reduced, while phosphorylated p53 protein expression was enhanced. Also, the decrease of MDM2 and the enhancement of GADD45a protein expression confirmed that dioscin treatment activated the p53 signaling pathway in Ishikawa cells. In mice tumor constructed from EC Ishikawa cells, WB results also showed that dioscin significantly increased p-p53 and GADD45a in p53 signaling pathway (Fig. 8B). Immunohistochemical results also showed enhanced expression of p-p53 protein in tumor tissues of the dioscin treated group, indicating that the anti-EC activity of dioscin was related to activation of p53 signaling pathway (Fig. 8C). The use of p53 inhibitor led to a decrease in p53 protein and a significant decrease in LC3II/LC3I, and the decreased autophagy protein rebounded after dioscin treatment. It was also confirmed that the use of p53 inhibitor pifithrin-α (PFT-α) was able to significantly inhibit the increase in autophagic flux induced by dioscin. Whereas after the p53 pathway was inhibited, caspase 3 did not change significantly, but was subsequently activated by dioscin treatment (Fig. 8D). This indicated that the dioscin induced p53 pathway was mainly involved in affecting the autophagy of Ishikawa cells and did not significantly dominate the process of apoptosis.

3.9 Relationship between dioscin-induced autophagy and apoptosis in Ishikawa cells

Dioscin increased the LC3II/LC3I protein ratio in Ishikawa cells, while the addition of the autophagy inhibitor 3-methyladenine (3-MA) attenuated the promoting effect of dioscin on LC3II expression (Fig. 9A), confirming that dioscin does act as an inducer of cellular autophagy. Meanwhile, compared with the dioscin treated group, the 3-MA + dioscin group showed a further

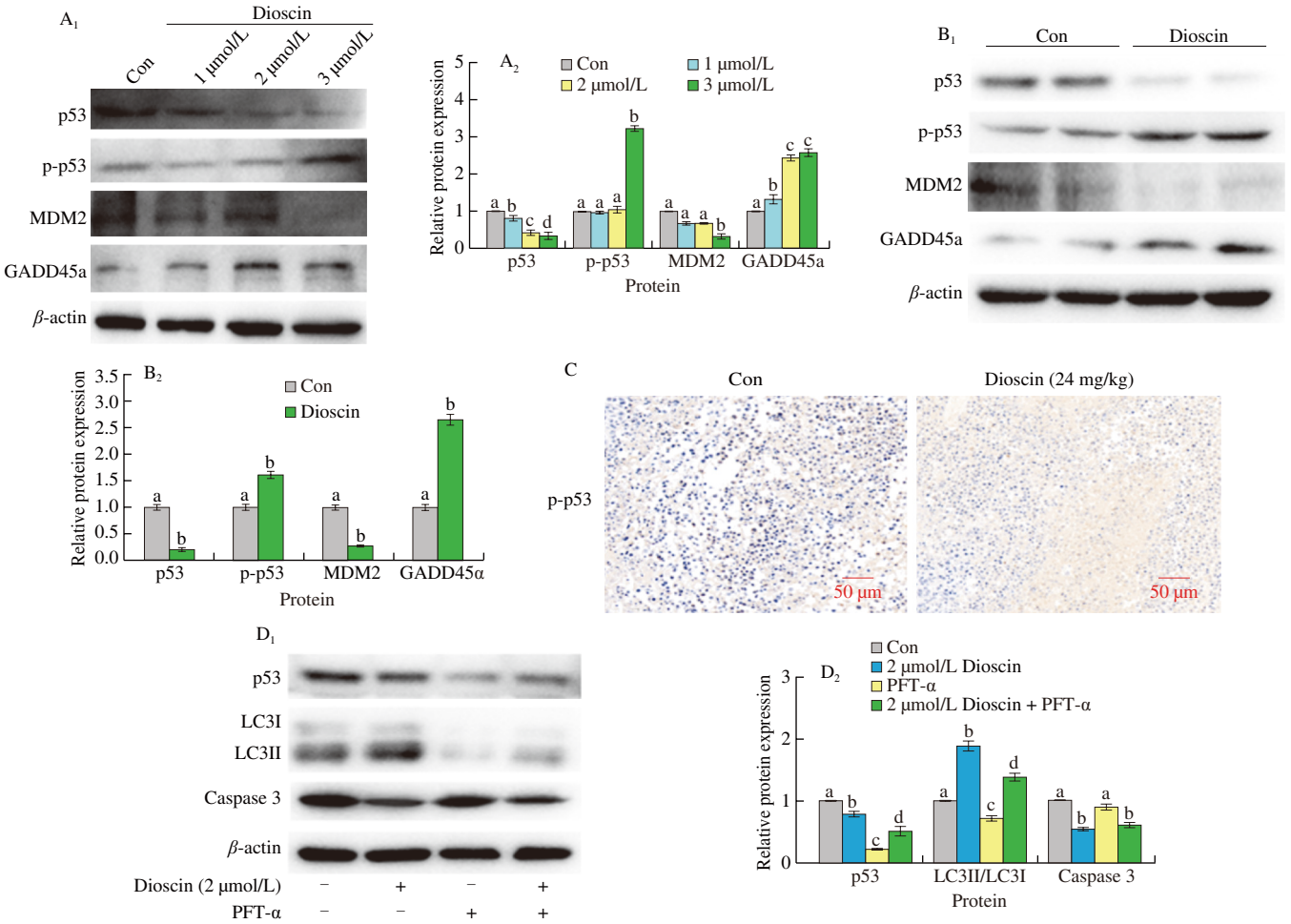


Fig. 8 Immunoblotting analysis for the protein of p53 signaling pathway. Protein expression profile and relative expression levels *in vitro* (A) and *in vivo* (B). (C) Immunohistochemistry for the detection of p-p53 expression in tumor sections. (D) Western blot analysis of p53, Caspase 3 and LC3 in Ishikawa cells after treatment of dioscin (2 μmol/L) and PFT-α.

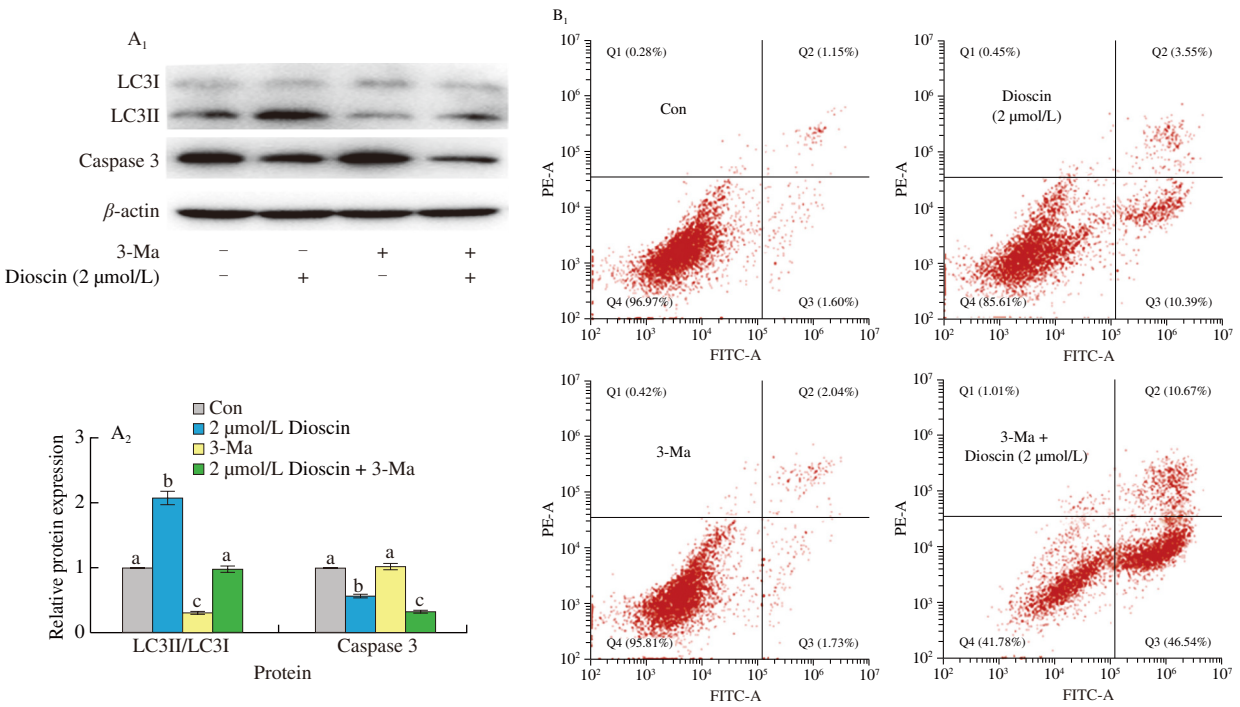


Fig. 9 Relationship between dioscin-induced autophagy and apoptosis in Ishikawa cells. (A) Western blot analysis of Caspase 3 and LC3 in Ishikawa cells after treatment of dioscin (2 μmol/L) and 3-Ma. (B) Representative images of Ishikawa cell apoptosis by flow cytometry after treatment of dioscin (2 μmol/L) and 3-Ma.

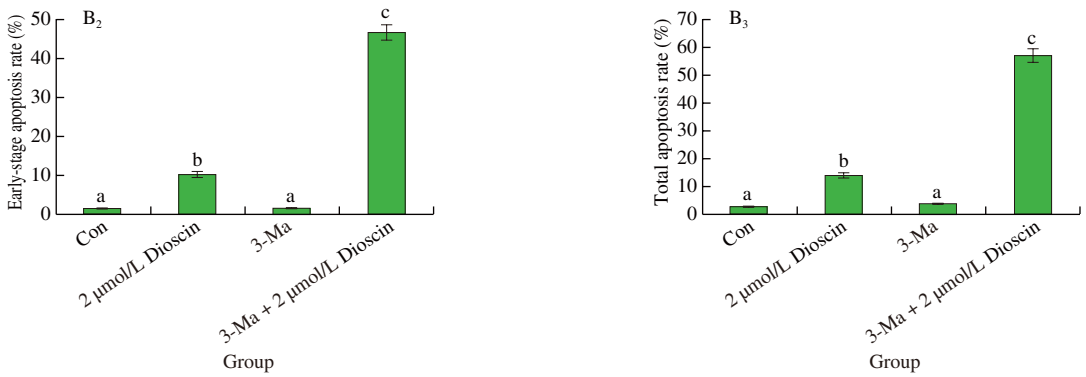


Fig. 9 (*Continued*)

decrease in the caspase-3 protein expression level, indicating that caspase-3 was activated to produce more shedders, suggesting that inhibition of autophagy could promote dioscin-induced apoptosis. Fig. 9B flow cytometric assay also revealed a higher percentage of apoptosis in 3-MA + dioscin treated group compared to dioscin treated group, indicating that the addition of 3-MA further promoted the onset of apoptosis. This also further suggested that there was a mutually antagonistic relationship between autophagy and apoptosis in Ishikawa cells.

3.10 Validation and regulation of miRNA and mRNA

Thus far, we have demonstrated that dioscin promoted apoptosis and autophagy in EC cells by inhibiting PI3K/AKT pathway, and dominated autophagy by activating the p53 signaling pathway. Subsequently, the expression of miRNAs and mRNAs was verified for the histological data *in vitro* cells and *in vivo* tumor tissues. As shown in Fig. 10A, the results of the validation assay showed that the miR-1246-p5_1ss17AG, miR-2887-1-p5, miR-6236-p3_1, and miR-19b-3p were enhanced, and miR-1260, miR-1180-5p_R-1, miR-1287-5p, and miR-10395 -3p showed a decreasing trend. The mRNA levels of *NGF*, *LAMA3*, *FGF2*, *IL4R*, and *GADD45A* genes were significantly increased, and mRNA levels of *TP53AIPI*, *PRLR*, and *LPAR3* genes were significantly decreased. The validation results of RT-qPCR *in vitro* and *in vivo* (Fig. 10B) demonstrated the consistency and reliability of histological results. To further elucidate the regulatory relationships between DEGs and DEMs dysregulated in PI3K/AKT and p53 signaling pathways, the miRNA-mRNA regulatory network relationship map between miRNAs and their potential target genes was established using Cytoscape software (Fig. 10C). Table 4 demonstrated that there was a negative regulatory relationship between 41 DEMs and 21 DEGs. The miRNAs and genes without negative regulatory relationships indicated the indirect interactions

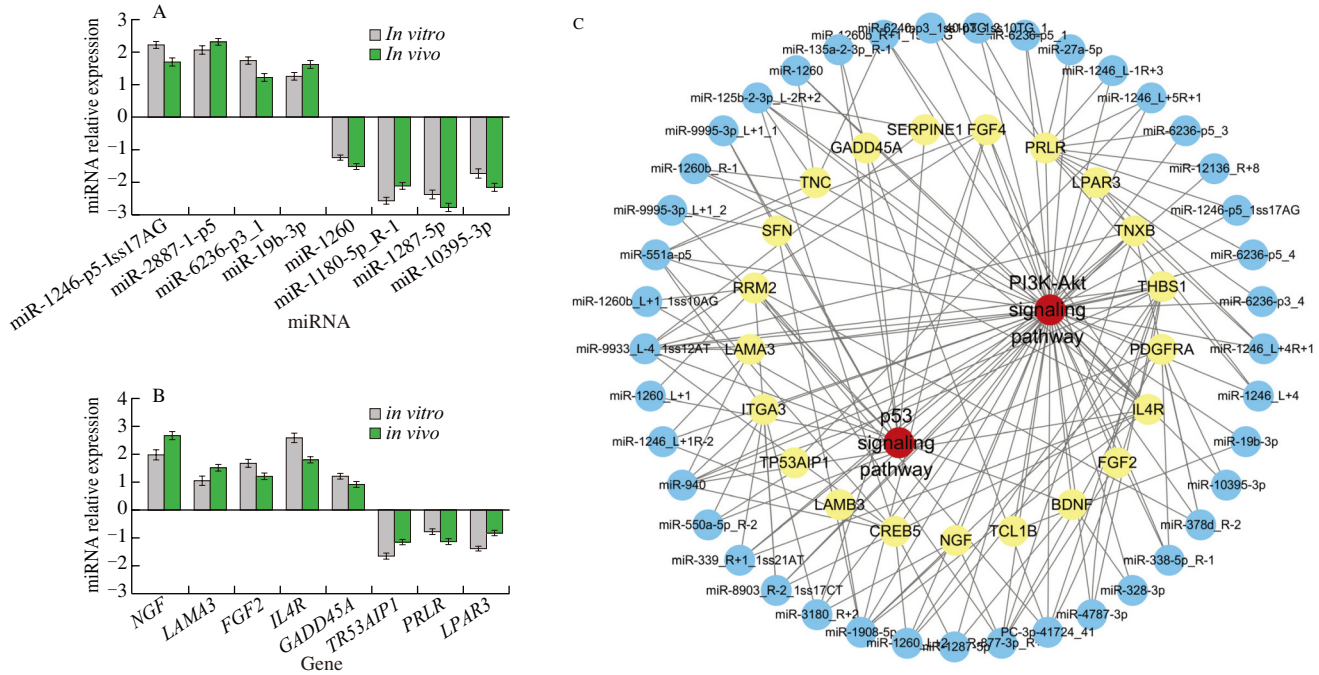


Fig. 10 Validation results of RT-qPCR *in vitro* and *in vivo* and regulation of miRNA and mRNA. Relative expression level of miRNAs (A) and mRNAs (B) with respect to the control group. (C) The miRNA-mRNA regulatory network relationship map.

between them. Among them, miR-1260, miR-1246, miR-940, and miR-9933 were more prominently linked, indicating that they may occupy key positions in the PI3K/AKT and p53 signaling pathways regulated by dioscin. The mining of these data provides a basis for exploring new therapeutic strategies for key miRNA regulation against EC.

Table 4
Regulatory relationship between genes and their corresponding DEMs of PI3K/AKT and p53 signaling pathways.

Genes	Regulation	miRNA	Regulation
TNC	Up	miR-1260b_R+1_1ss9AG	Down
		miR-1260	Down
		miR-125b-2-3p_L-2R+2	Down
		miR-1260b_R-1	Down
		miR-551a-p5	Down
LAMA3	Up	miR-9933_L-4_1ss12AT	Down
		miR-1246_L+1R-2	Down
		miR-940	Down
ITGA3	Up	miR-550a-5p_R-2p	Down
		miR-339_R+1_1ss21AT	Down
		miR-8903_R-2_1ss17CT	Down
		miR-940	Down
		miR-3180_R+2	Down
		miR-551a-p5	Down
LAMB3	Up	miR-1908-5p	Down
CREB5	Up	miR-1246_L+1R-2	Down
		miR-1260_L+2	Down
		miR-9933_L-4_1ss12AT	Down
		miR-125b-2-3p_L-2R+2	Down
		miR-940	Down
		miR-551a-p5	Down
		miR-1287-5p	Down
NGF	Up	miR-1908-5p	Down
		miR-3180_R+2	Down
		miR-877-3p_R+1	Down
THBS1	Up	PC-3p-41724_41	Down
		miR-1260_L+2	Down
		miR-9933_L-4_1ss12AT	Down
		miR-4787-3p	Down
		miR-940	Down
BDNF	Up	miR-9933_L-4_1ss12AT	Down
		miR-1287-5p	Down
		miR-328-3p	Down
FGF2	Up	miR-877-3p_R+1	Down
IL4R	Up	miR-8903_R-2_1ss17CT	Down
		miR-125b-2-3p_L-2R+2	Down
		miR-1908-5p	Down
		miR-940	Down
		miR-1260b_R+1_1ss9AG	Down
		miR-1260	Down
		miR-1260b_R-1	Down
		miR-339_R+1_1ss21AT	Down
PDGFRA	Up	miR-1908-5p	Down
		miR-338-5p_R-1	Down
		miR-378d_R-2	Down
		miR-550a-5p_R-2	Down
		miR-877-3p_R+1	Down
		miR-10395-3p	Down
TCL1B	Up	miR-940	Down
TNXB	Up	miR-8903_R-2_1ss17CT	Down

Table 4 (*Continued*)

Genes	Regulation	miRNA	Regulation
		miR-9933_L-4_1ss12AT	Down
		miR-378d_R-2	Down
		miR-877-3p_R+1	Down
		miR-339_R+1_1ss21AT	Down
FGF4	Up	miR-9933_L-4_1ss12AT	Down
		miR-1908-5p	Down
		miR-3180_R+2	Down
		miR-338-5p_R-1	Down
		miR-551a-p5	Down
SERPINE1	Up	miR-9933_L-4_1ss12AT	Down
		miR-125b-2-3p_L-2R+2	Down
GADD45A	Up	PC-3p-41724_41	Down
		miR-135a-2-3p_R-1	Down
SFN	Up	miR-1908-5p	Down
		miR-9995-3p_L+1_1	Down
		miR-9995-3p_L+1_2	Down
RRM2	Up	miR-1260b_L+1_1ss10AG	Down
		miR-1260_L+1	Down
		PC-3p-41724_41	Down
		miR-877-3p_R+1	Down
		miR-551a-p5	Down
		miR-8903_R-2_1ss17CT	Down
		miR-378d_R-2	Down
TP53AIP1	Down	miR-1246_L+5R+1	Up
LPAR3	Down	miR-1246_L+4	Up
		miR-1246_L+4R+1	Up
PRLR	Down	miR-6236-p3_4	Up
		miR-6236-p5_4	Up
		miR-1246-p5_1ss17AG	Up
		miR-12136_R+8	Up
		miR-6236-p5_3	Up
		miR-1246_L+4	Up
		miR-1246_L+4R+1	Up
		miR-1246_L+5R+1	Up
		miR-1246_L-1R+3	Up
		miR-27a-5p	Up
		miR-6236-p5_1	Up
		miR-6240-p3_1ss10TG_1	Up
		miR-6240-p3_1ss10TG_2	Up

4. Discussion

In our present study, the dioscin component was extracted and purified from PS and structurally characterized. Several studies have indicated that dioscin exhibit remarkable anti-cancer, anti-inflammatory, immunomodulatory, hypolipidemic, antiviral, antifungal, and anti-allergic effects[21,29,41]. For the past few years, numerous studies have focused on exploring dioscin against a variety of cancers. As a natural product, dioscin has been reported to have certain inhibitory effects on breast[42], stomach[41], lung[15], and liver cancers[14], acute myeloid leukemia[43] as well as melanoma[44]. In this study, we preliminarily determined the anti-EC activity of dioscin by inhibiting Ishikawa cell viability and the tumor growth in mice. Through the review of previously targeted pathways and molecular mechanisms, dioscin was found to exert its anti-cancer effects by triggering DNA damage, inducing cell cycle arrest, increasing apoptosis rate, activating cell autophagy, inhibiting tumor stem cells,

stimulating mitochondrial damage, increasing intracellular reactive oxygen species accumulation, and Ca^{2+} release[14,21,42,45]. Our past findings have explored the dioscin induced apoptosis through cycle block and mitochondria-related pathways[17], but the specific anti-cancer mechanism of dioscin action in EC still remains elusive. Dioscin-induced Ishikawa cell death was a very complex biological process involving differential expression of a large number of genes and regulation of multiple biological factors such as transcription factors and miRNAs. Therefore, we used high-throughput sequencing to initially explore the possible regulatory mechanisms of dioscin against EC from the perspective of miRNAomics. Then, based on multi-omics data and *in vitro* and *in vivo* models, we validated multiple signaling targets and further screened the functional miRNAs. The enrichment analysis of histological data indicated that dioscin exerted anti-EC effects via PI3K/AKT and p53 pathway, two interactive signaling targets of apoptosis and autophagy.

The natural compounds are reported to involve multiple regulatory pathways and molecular mechanisms. Apoptosis, as the first programmed cell death procedure to be identified and its regulatory network have gradually been recognized[46]. Caspase proteins, a group of structurally similar cystatin proteases found in the cytoplasm, are closely related to apoptosis[47]. And the Bcl-2 protein family, which contains pro-apoptotic and anti-apoptotic proteins, also triggers a series of apoptotic events[48]. In this study, we found that there was a significant concentration-dependent increase of Bad protein in Ishikawa cells with the increasing concentration of dioscin administration. The tumor protein results indicated a significant decrease in PARP and Bcl-2 proteins, and a significant increase in the apoptosis marker protein of c-PARP. Immunohistochemical results showed a decrease in caspase 9 intensity in the dioscin-treated group, suggesting activation. These results suggested that dioscin had a better effect of promoting apoptosis in EC Ishikawa cells. Furthermore, apoptosis was not the only autonomously ordered death process that was controlled by a specific base. As research has progressed, autophagy occurrence in bioactive components used as functional foods has been explored as a co-regulator of cell death with apoptosis[49]. Initially, autophagy was thought to play an important role only as a cellular self-protection mechanism against nutrient deficiency and removal of damaged organelles and macromolecules from the cytoplasm. But there is growing evidence that autophagy has contributed its own power in tumor development[50]. It has been found that activation of autophagy significantly inhibited the proliferation of a variety of cancer cells[20-23,38]. Furthermore, emerging evidence suggested that autophagy and apoptosis triggered by the regulation of multiple signaling pathways were involved in tumor suppression in EC[23-25,51-52]. The formation of autophagic lysosomes was critical in the autophagic process. We detected a significant increase in autophagic vesicles in Ishikawa cells after dioscin treatment, suggesting that dioscin promoted autophagic activity in Ishikawa cells. The increase in red light intensity in LC3 staining also tentatively suggested that dioscin regulated activities related to cellular autophagy. LC3 was one of the signature proteins of autophagy, and LC3 translocated from the cytoplasmic type (LC3I) to the autophagosomal membrane (LC3II) during autophagy regulation[38]. Beclin-1 and p62 were also important markers of autophagy, and both of them can clearly reflect the level of autophagy in cells. Beclin-1 protein expression level positively regulated autophagy, while p62 protein negatively correlated with autophagy[53]. The detection of protein levels revealed that the LC3II/LC3I ratio and Beclin-1 levels increased significantly with the increase of dioscin treatment concentration, and the p62 protein expression level decreased significantly. Immunohistochemical results showed that the intensity of Beclin-1 was enhanced in the dioscin-treated tumor sample group. All these results suggested that dioscin induced the occurrence of cellular autophagy. We hypothesized that dioscin activated the process of autophagy and apoptosis. Similar results were seen in human EC cell lines Ishikawa, HEC-1A and RL95-2 cells, where apoptosis and autophagy were induced by Isoliquiritigenin[54].

Different from the unidirectional regulation of cell death by apoptosis, in some cases, autophagy inhibited apoptosis and was responsible for the cell survival pathway[55]. However, autophagy itself also elicited cell death acting in conjunction with apoptosis or as a backup mechanism to induce cell death in the presence of defective apoptosis[50]. Apoptosis and autophagy were interrelated and mutually regulated. Although autophagy and apoptosis are significantly different in terms of metabolic pathways and morphology, their signaling pathways were found to be inextricably linked. The multiple interaction modes of apoptosis and autophagy necessarily shared common signal transduction and regulatory proteins. Based on our histological results, we focused on exploring the dual regulatory roles of PI3K/AKT and p53 in dioscin induced autophagy and apoptosis in Ishikawa cells. As one of the classical tumors signaling pathways, PI3K/AKT has been proven to exert anti-tumor effects by regulating both apoptosis and autophagy[20,23,28,56]. When PI3K binds to the growth factor receptor, it can activate the downstream AKT and affect the activity of downstream substrates, thus regulating cell proliferation, apoptosis and autophagy. We found that the relative expression of p-PI3K, p-AKT and p-mTOR proteins in Ishikawa cells by dioscin was reduced, suggesting that dioscin could inhibit PI3K/AKT/mTOR signaling pathway in Ishikawa cells. As a downstream regulator of PI3K/AKT, mTOR regulated a number of life activities, especially played an important pivotal role in the occurrence of apoptosis and autophagy. Studies have revealed that mTOR negatively modulated autophagy, while having a dual effect on regulating cell apoptosis[26,42]. Our experiments showed that mTOR exhibited negative feedback regulation on both autophagy and apoptosis. The addition of AKT inhibitors and activators reinforced that dioscin induced apoptosis and autophagy in Ishikawa cells, associated with inhibition of PI3K/AKT/mTOR signaling pathway expression. The results of Liu et al.[57] elucidated that mTOR could be a target for the treatment of progestin-resistant EC. The results of Lin et al.[36] similarly demonstrated that regulation of the PI3K/AKT/mTOR signaling pathway promoted autophagy in the Ishikawa EC cell line. Another study demonstrated induction of EC cell apoptosis and autophagy through inhibition of PI3K/AKT/mTOR pathway by establishing xenograft model experiments[23].

p53, widely known as the “guardian of the genome”, is a tumor suppressor gene. The p53 protein signaling pathway can respond to a variety of different cellular stress signals leading to different types of DNA damage and disruption of DNA template integrity to suppress cancer. Once activated, p53 reflects a complex signal transduction network to play a single or interactive role in inducing apoptosis and regulating autophagy[58-59]. In this study, we found that the expression of p53 and MDM2 proteins was decreased, while the expression of

p-p53 and GADD45a proteins was increased after treatment with dioscin, suggesting the activation of p53 signaling pathway. Therefore, we have reason to believe that dioscin can induce increased levels of cellular autophagy by activating AMPK and inhibiting mTOR activity. As a convergence point of multiple signaling pathways, mTOR mainly participated in cell apoptosis, energy metabolism, and the growth of various tumors[21]. Its inhibition in the regulation of autophagic process could reduce the level of ULK1, a key regulatory protein of autophagy, which in turn promoted Beclin-1 expression and LC3I to LC3II conversion, thus enhancing the level of autophagy in EC. This was consistent with the electron microscopic observations and the trend of p-p53 immunohistochemistry results. The use of p53 inhibitor revealed that the dioscin-regulated p53 pathway was mainly involved in affecting autophagy in Ishikawa cells without significantly dominating the process of apoptosis. Interestingly, p53 has been shown to be a crossroads between autophagy and apoptosis. On the one hand, p53 regulated Bcl-2-related proteins and signaling pathways to promote apoptosis[60], and on the other hand, p53 harmonized the development of autophagy in tumor cells. Induction of autophagy in HCT116 colon cancer cells was p53-dependent[38]. It has also been reported that apoptosis was attenuated, and autophagy impairment was improved by targeting the p53 pathway in AC16 cell line[61]. Johnson et al.[62] showed that inhibition of p53 resulted in reducing apoptosis and increasing autophagy in H9C2 cardiomyocytes.

It was shown that autophagy has a dual role in the prevention and treatment of EC. On the one hand autophagy negatively regulated EC and autophagy inducers may contribute to the chemoprevention of EC. Conversely, autophagy is reported to promote EC[22]. This idea led us to probe the relationship between dioscin-induced cellular autophagy and apoptosis using the autophagy inhibitor 3-Ma. It was found that inhibition of autophagy promoted dioscin-induced apoptosis. The addition of the autophagy inhibitor 3-Ma further promoted apoptosis. It has been suggested that chemotherapy-induced autophagy triggered chemoresistance in EC cells, so the combination of chemotherapy and autophagy inhibitors may be an effective therapeutic option for EC patients[63]. Song et al.[64] reported that the combination of Tanshinone IIA with 3-MA resulted in enhanced Tanshinone IIA-induced apoptosis in human monocytic leukemia cell line THP-1 cells. The combination of compound with autophagy inhibitors acting on apoptosis can be a novel and effective combination therapy with potential application in clinical treatment.

In tumor therapy, miRNA-mediated gene expression regulated by natural compounds or phytochemicals represent a potential molecular target in therapeutic clinical approaches[61]. Validation of the histological results demonstrated the reliability of enrichment analysis based on histological data. Regulatory networks were also analyzed for relevant hub miRNAs and genes. Apoptosis and autophagy were also regulated by other interacting pathways and multiple modulatory elements such as miRNAs and long-stranded non-coding RNAs[24]. Here, we explored the possible connection between apoptosis and autophagy and PI3K/AKT and p53 pathways in dioscin treated EC Ishikawa cells. The specific in-depth interactions between apoptosis and autophagy and other regulatory pathways or molecules need to be further verified by subsequent experiments such as using knockdown techniques.

On the other hand, it has long been established in the field of molecular biology that tumors as a genetic disease create aberrations in the genome through DNA nucleotide sequence alterations. And the regulation of the genome through epigenetic alterations adds complexity. Increasingly, studies have shown that epigenetics, which do not depend on DNA sequence alterations leading to changes in gene expression levels, are revealed to play an important role in tumor formation, intersecting with genetic mechanisms that exist together to promote tumor formation. To understand whether dioscin induced apoptosis and autophagy mechanisms in relation to epigenetic regulation, we further evaluated the methylation status of genes (AKT, p53, caspase 3, and LC3B) in cells *in vitro* as well as in mouse tumor tissues *in vivo*. As shown in Fig. S1, the promoter regions of AKT, p53, and LC3B genes were completely unmethylated in the Ishikawa cell line as well as in the tumor tissues of endometrial cancer mice, and no methylation status was found. Methylation of the promoter region of caspase 3 gene in cells and tumor tissues

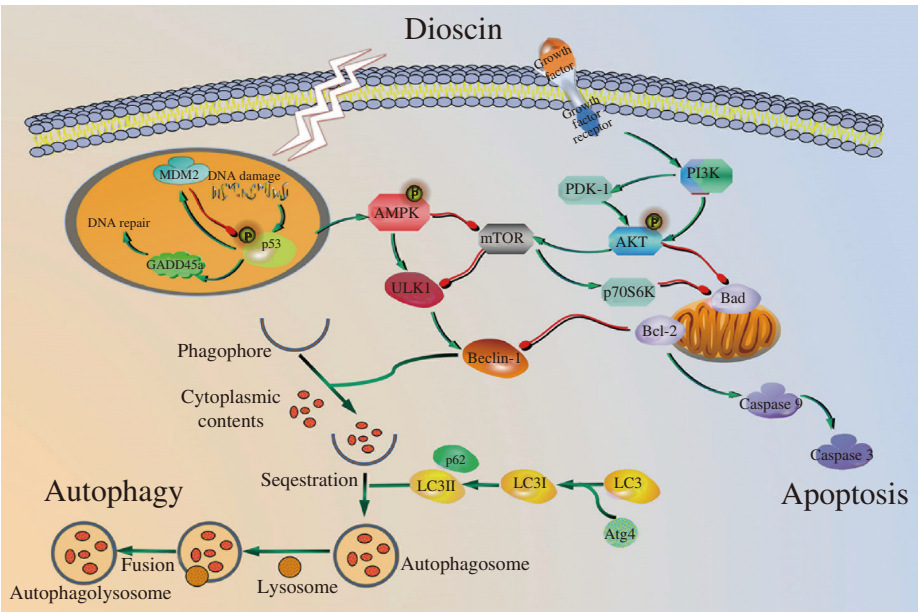


Fig. 11 Schematic representation of dioscin to induce apoptosis and autophagy in Ishikawa cells.

suggested a possible involvement in the development and progression of endometrial cell carcinoma. Furthermore, no alteration in the methylation status of the promoter regions of these 4 genes was found *in vitro* and *in vivo* levels after dioscin treatment compared to the control group, and our results tentatively suggested that the mechanism of dioscin in fighting endometrial cancer may not be closely related to epigenetic regulatory mechanisms. In addition, the epigenetic mechanisms of endometrial cancer development and the relationship between nutritional epigenetics and dioscin function also need to be investigated in more depth and comprehensively by whole genome DNA methylation sequencing.

5. Conclusion

In conclusion, at first, we determined the anti-EC activity of dioscin by suppressing cellular viability and tumor growth, which was followed by uncovering the signaling targets of dioscin-induced apoptosis and autophagy based on miRNA omics data enrichment analysis. The interactive regulation of PI3K/AKT and p53 signaling pathways on apoptosis and autophagy in Ishikawa cells was clarified by *in vivo* and *in vitro* validation experiments. The results suggested that dioscin promoted apoptosis and autophagy in Ishikawa cells by inhibiting PI3K/AKT/mTOR signaling pathway and dominated autophagy by activating p53 signaling pathway (Fig. 11). And after the addition of the autophagy inhibitor 3-Ma, the level of dioscin-induced apoptosis was further promoted. Ultimately, multiple signaling targets were validated and functional miRNAs were further screened to provide a basis for exploring the new therapeutic strategies for anti-EC activity of dioscin. This study presents the multiple signaling targets and potential molecular mechanisms of the anticancer effects of dioscin with a particular emphasis on EC.

Conflict of interest

Zhaojun Wei is an editorial board member for *Food Science and Human Wellness* and was not involved in the editorial review or the decision to publish this article. There is none to declare.

Acknowledgments

This work was supported by the National Key Research & Development Program of China (2022YFF1100305), the National Natural Science Foundation of Ningxia Province (2021AAC02019, 2022AAC03230), and the Key research and development projects in Ningxia province (2021BEF02013).

Appendix A. Supplementary data

Supplementary data associated with this article can be found, in the online version, at http://doi.org/10.26599/FSHW.2022.9250209.

References

[1] J. Lortet-Tieulent, J. Ferlay, F. Bray, et al., International patterns and trends in endometrial cancer incidence, 1978−2013, J. Natl. Cancer Inst. 110 (2018) 354-361. https://doi.org/10.1093/jnci/djx214.

[2] R.L. Siegel, K.D. Miller, H.E. Fuchs, et al., Cancer statistics, 2021, CA-Cancer J. Clin. 71 (2021) 7-33. https://doi.org/10.3322/caac.21654.

[3] S.J. Henley, E.M. Ward, S. Scott, et al., Annual report to the nation on the status of cancer, part I: national cancer statistics, Cancer 126 (2020) 2225-2249. https://doi.org/10.1002/cncr.32802.

[4] H. Sung, R.L. Siegel, P.S. Rosenberg, et al., Emerging cancer trends among young adults in the USA: analysis of a population-based cancer registry, Lancet Public Health 4 (2019) e137-e147. https://doi.org/10.1016/S2468-2667(18)30267-6.

[5] E.J. Crosbie, S.J. Kitson, J.N. McAlpine, et al., Endometrial cancer, Lancet 399 (2022) 1412-1428. https://doi.org/10.1016/S0140-6736(22)00323-3.

[6] S. Wang, G. Li, X. Zhang, et al., Structural characterization and antioxidant activity of *Polygonatum sibiricum* polysaccharides, Carbohydr. Polym. 291 (2022) 119524. https://doi.org/10.1016/j.carbpol.2022.119524.

[7] Y. Xie, Z. Jiang, R. Yang, et al., Polysaccharide-rich extract from *Polygonatum sibiricum* protects hematopoiesis in bone marrow suppressed by triple negative breast cancer, Biomed. Pharmacother. 137 (2021) 111338. https://doi.org/10.1016/j.biopha.2021.111338.

[8] L.X. Li, X. Feng, M.T. Tao, et al., Benefits of neutral polysaccharide from rhizomes of *Polygonatum sibiricum* to intestinal function of aged mice, Front. Nutr. 9 (2022) 992102. https://doi.org/10.3389/fnut.2022.992102.

[9] Y. He, L. Huang, P. Jiang, et al., Immunological regulation of the active fraction from *Polygonatum sibiricum* F. Delaroche based on improvement of intestinal microflora and activation of RAW264.7 cells, J. Ethnopharmacol. 293 (2022) 115240. https://doi.org/10.1016/j.jep.2022.115240.

[10] K. Maharajan, Q. Xia, X. Duan, et al., Therapeutic importance of Zishen Yutai Pill on the female reproductive health: a review, J. Ethnopharmacol. 281 (2021) 114523. https://doi.org/10.1016/j.jep.2021.114523.

[11] S.N.S. Lamardi, S. Ghambariyan, M.R.S. Ardekani, et al., Major phytosteroid from *Polygonatum orientale* Desf. Rhizome, J. Pharm. Health Sci. 5 (2017) 43-49.

[12] A. Tariq, S. Mussarat, M. Adnan, et al. Review on ethnomedicinal, phytochemical and pharmacological evidence of Himalayan anticancer plants, J. Ethnopharmacol. 164 (2015) 96-119. https://doi.org/10.1016/j.jep.2015.02.003.

[13] D.P. Xu, C.Y. Hu, Y. Zhang, Two new steroidal saponins from the rhizome of *Polygonatum sibiricum*, J. Asian Nat. Prod. Res. 11 (2009) 1-6. https://doi.org/10.1080/10286020802513681.

[14] Y.S. Zhang, Y.L. Ma, K. Thakur, et al., Molecular mechanism and inhibitory targets of dioscin in HepG2 cells, Food Chem. Toxicol. 120 (2018) 143-154. https://doi.org/10.1016/j.fct.2018.07.016.

[15] P. Xi, Y. Niu, Y. Zhang, et al., The mechanism of dioscin preventing lung cancer based on network pharmacology and experimental validation, J. Ethnopharmacol. 292 (2022) 115138. https://doi.org/10.1016/j.jep.2022.115138.

[16] S. Wu, F. Zhao, J. Zhao, et al., Dioscin improves postmenopausal osteoporosis through inducing bone formation and inhibiting apoptosis in ovariectomized rats, Biosci. Trends 13 (2019) 394-401. https://doi.org/10.5582/bst.2019.01186.

[17] X.L. Li, R.H. Ma, Z.J. Ni, et al., Dioscin inhibits human endometrial carcinoma proliferation via G0/G1 cell cycle arrest and mitochondrial-dependent signaling pathway, Food Chem. Toxicol. 148 (2021) 111941. https://doi.org/10.1016/j.fct.2020.111941.

[18] S.I. Nuñez-Olvera, D. Gallardo-Rincón, J. Puente-Rivera, et al., Autophagy machinery as a promising therapeutic target in endometrial cancer, Front. Oncol. 9 (2019) 1326. https://doi.org/10.3389/fonc.2019.01326.

[19] Z. Zhang, K. Han, C. Wang, et al., Dioscin protects against Aβ1-42 oligomers-induced neurotoxicity via the function of SIRT3 and autophagy, Chem. Pharm. Bull. 68 (2020) 717-725. https://doi.org/10.1248/cpb.c20-00046.

[20] M.J. Hsieh, T.L. Tsai, Y.S. Hsieh, et al., Dioscin-induced autophagy mitigates cell apoptosis through modulation of PI3K/Akt and ERK and JNK signaling pathways in human lung cancer cell lines, Arch. Toxicol. 87 (2013) 1927-1937. https://doi.org/10.1007/s00204-013-1047-z.

[21] H. Li, B. Pang, B. Nie, et al., Dioscin promotes autophagy by regulating the AMPK-mTOR pathway in ulcerative colitis, Immunopharmacol. Immunotoxicol. 44 (2022) 238-246. https://doi.org/10.1080/08923973.2022.2037632.

[22] S. Deng, M.K. Shanmugam, A.P. Kumar, et al., Targeting autophagy using natural compounds for cancer prevention and therapy, Cancer 125 (2019) 1228-1246. https://doi.org/10.1002/cncr.31978.

[23] L. Zhou, S. Li, J. Sun, Ginkgolic acid induces apoptosis and autophagy of endometrial carcinoma cells via inhibiting PI3K/Akt/mTOR pathway *in vivo* and *in vitro*, Hum. Exp. Toxicol. 40 (2021) 2156-2164. https://doi.org/10.1177/09603271211023789.

[24] F. Zhang, Y.Y. Zhang, R.H. Ma, et al., Multi-omics reveals the anticancer mechanism of asparagus saponin-asparanin A on endometrial cancer Ishikawa cells, Food Funct. 12 (2021) 614-632. https://doi.org/10.1039/d0fo02265a.

[25] X. Ran, J. Yang, C. Liu, et al., MiR-218 inhibits HMGB1-mediated autophagy in endometrial carcinoma cells during chemotherapy, Int. J. Clin. Exp. Pathol. 8 (2016) 6617-6626.

[26] Z. Zhuo, H. Yu, miR-205 inhibits cell growth by targeting AKT-mTOR signaling in progesterone-resistant endometrial cancer Ishikawa cells, Oncotarget 8 (2017) 28042-28051. https://doi.org/10.18632/oncotarget.15886.

[27] J. Wang, X.X. Zhang, Z.J. Ni, et al., The anti-cancerous mechanism of licochalcone A on human hepatoma cell HepG2 based on the miRNA omics, Food Sci. Hum. Wellness 12 (2023) 1136-1148. https://doi.org/10.1016/j.fct.2021.112096.

[28] F. Zhang, Y.Y. Zhang, Y.S. Sun, et al., Asparanin A from *Asparagus officinalis* L. induces G0/G1 cell cycle arrest and apoptosis in human endometrial carcinoma Ishikawa cells via mitochondrial and PI3K/AKT signaling pathways, J. Agric. Food Chem. 68 (2020) 213-224. https://doi.org/10.1021/acs.jafc.9b07103.

[29] Z. Zhang, J. Wu, C. Teng, et al., Safranal treatment induces Sirt1 expression and inhibits endoplasmic reticulum stress in mouse chondrocytes and alleviates osteoarthritis progression in a mouse model, J. Agric. Food Chem. 70 (2020) 9748-9759. https://doi.org/10.1021/acs.jafc.2c01773.

[30] X.L. Li, X.X. Zhang, R.H. Ma, et al., Integrated miRNA and mRNA omics reveal dioscin suppresses migration and invasion via MEK/ERK and JNK signaling pathways in human endometrial carcinoma *in vivo* and *in vitro*, J. Ethnopharmacol. 303 (2022) 116027. https://doi.org/10.1016/j.jep.2022.116027.

[31] L. Zheng, L. Yin, L. Xu, et al., Protective effect of dioscin against thioacetamide-induced acute liver injury via FXR/AMPK signaling pathway *in vivo*, Biomed. Pharmacother. 97 (2018) 481-488. https://doi.org/10.1016/j.biopha.2017.10.153.

[32] Q. Ding, W. Zhang, C. Cheng, et al., Dioscin inhibits the growth of human osteosarcoma by inducing G2/M-phase arrest, apoptosis, and GSDME-dependent cell death *in vitro* and *in vivo*, J. Cell Physiol. 235 (2020) 2911-2924. https://doi.org/10.1002/jcp.29197.

[33] X. Zhao, L. Xu, L. Zheng, et al., Potent effects of dioscin against gastric cancer *in vitro* and *in vivo*, Phytomedicine 23 (2016) 274-282. https://doi.org/10.1016/j.phymed.2016.01.012.

[34] J.Wang, C.Y. Wang, Integrated miRNA and mRNA omics reveal the anti-cancerous mechanism of licochalcone B on human hepatoma cell HepG2, Food Chem. Toxicol. 150 (2021) 112096. https://doi.org/10.1016/j.fct.2021.112096.

[35] F. Zhang, Z.J. Ni, L. Ye, et al., Asparanin A inhibits cell migration and invasion in human endometrial cancer via Ras/ERK/MAPK pathway, Food Chem. Toxicol. 150 (2021) 112036. https://doi.org/10.1016/j.fct.2021.112036.

[36] Q. Lin, S. Li, N. Jiang, et al., Inhibiting NLRP3 inflammasome attenuates apoptosis in contrast-induced acute kidney injury through the upregulation of HIF1A and BNIP3-mediated mitophagy, Autophagy 17 (2021) 2975-2990. https://doi.org/10.1080/15548627.2020.1848971.

[37] Y.S. Sun, K. Thakur, F. Hu, et al., Icariside II suppresses cervical cancer cell migration through JNK modulated matrix metalloproteinase-2/9 inhibition *in vitro* and *in vivo*, Biomed. Pharmacother. 125 (2020) 110013. https://doi.org/10.1016/j.biopha.2020.110013.

[38] Y. Zhou, X. Zhou, X. Huang, et al., Lysosome-mediated cytotoxic autophagy contributes to tea polysaccharide-induced colon cancer cell death via mTOR-TFEB signaling, J. Agric. Food Chem. 69 (2021) 686-697. https://doi.org/10.1021/acs.jafc.0c07166.

[39] S.S. Hussain, F. Zhang, Y.Y. Zhang, et al., Stevenleaf from *Gynostemma pentaphyllum* inhibits human hepatoma cell (HepG2) through cell cycle arrest and apoptotic induction, Food Sci. Hum. Wellness 9 (2020) 295-303. https://doi.org/10.1016/j.fshw.2020.04.011.

[40] S. Man, W. Gao, Y. Zhang, et al., Characterization of steroidal saponins in saponin extract from *Paris polyphylla* by liquid chromatography tandem multi-stage mass spectrometry, Anal. Bioanal. Chem. 395 (2009) 495-505. https://doi.org/10.1007/s00216-009-2987-2.

[41] X. Tao, L. Yin, L. Xu, et al., Dioscin: a diverse acting natural compound with therapeutic potential in metabolic diseases, cancer, inflammation and infections, Pharmacol. Res. 137 (2018) 259-269. https://doi.org/10.1016/j.phrs.2018.09.022.

[42] W.O. Chae, G.D. Kim, Dioscin decreases breast cancer stem-like cell proliferation via cell cycle arrest by modulating p38 mitogen-activated protein kinase and AKT/mTOR signaling pathways, J. Cancer Prev. 26 (2021) 183-194. https://doi.org/10.15430/JCP.2021.26.3.183.

[43] S.H. Chan, P.H. Liang, J.H. Guh, An integrated approach to elucidate signaling pathways of dioscin-induced apoptosis, energy metabolism and differentiation in acute myeloid leukemia, Naunyn Schmiedebergs Arch. Pharmacol. 391(2018) 587-602. https://doi.org/10.1007/s00210-018-1484-6.

[44] Y.X. Liu, B.W. Xu, X.D. Niu, et al., Inhibition of Src/STAT3 signaling-mediated angiogenesis is involved in the anti-melanoma effects of dioscin, Pharmacol. Res. 175 (2022) 105983. https://doi.org/10.1016/j.phrs.2021.105983.

[45] H. Teng, Y. Qian, X. Fan, et al., Nutritional properties of Europen eel (*Anguilla anguilla*) bone peptide-calcium and its apoptosis effect on Caco-2 cells, Food Sci. Hum. Wellness 11 (2022) 1482-1490. https://doi.org/10.1016/j.fshw.2022.06.005.

[46] G. Majno, I. Joris, Apoptosis, oncosis, and necrosis. an overview of cell death, Am. J. Pathol. 146 (1995) 3-15.

[47] J. Yuan, A. Najafov, B.F. Py, Roles of caspases in necrotic cell death, Cell 167 (2016) 1693-1704. https://doi.org/10.1016/j.cell.2016.11.047.

[48] A. Ashkenazi, W.J. Fairbrother, J.D. Leverson, et al., From basic apoptosis discoveries to advanced selective BCL-2 family inhibitors, Nat. Rev. Drug Discov. 16 (2017) 273-284. https://doi.org/10.1038/nrd.2016.253.

[49] J. Xie, J. Liang, N. Chen, Autophagy-associated signal pathways of functional foods for chronic diseases, Food Sci. Hum. Wellness 8 (2019) 25-33. https://doi.org/10.1016/j.fshw.2019.03.002.

[50] D. Denton, S. Kumar, Autophagy-dependent cell death, Cell Death Differ. 26 (2019) 605-616. https://doi.org/10.1038/s41418-018-0252-y.

[51] R.H. Ma, Z.J. Ni, F. Zhang, et al., 6-Shogaol mediated ROS production and apoptosis via endoplasmic reticulum and mitochondrial pathways in human endometrial carcinoma Ishikawa cells, J. Funct. Foods 74 (2020) 104178. https://doi.org/10.1016/j.jff.2020.104178.

[52] Y.C. Liang, Q. Zhong, R.H. Ma, et al., Apigenin, a natural flavonoid, promotes autophagy and ferroptosis in human endometrial carcinoma (EC) Ishikawa cells *in vitro* and *in vivo*, Food Sci. Hum. Wellness 12 (2023) 2242-2251. https://doi.org/10.1016/j.fshw.2023.03.044.

[53] R. Mathew, C.M. Karp, B. Beaudoin, et al., Autophagy suppresses tumorigenesis through elimination of p62, Cell 137 (2009) 1062-1075. https://doi.org/10.1016/j.cell.2009.03.048.

[54] C.H. Wu, H.Y. Chen, C.W. Wang, et al., Isoliquiritigenin induces apoptosis and autophagy and inhibits endometrial cancer growth in mice, Oncotarget 7 (2016) 73432-73447. https://doi.org/10.18632/oncotarget.12369.

[55] Q. Li, Y. Yin, Y. Zheng, et al., Inhibition of autophagy promoted high glucose/ROS-mediated apoptosis in ADSCs, Stem Cell Res. Ther. 9 (2018) 289. https://doi.org/10.1186/s13287-018-1029-4.

[56] S.Y. Kim, H.K. Yi, B.S. Yun, et al., The extract of the immature fruit of *Poncirus trifoliata* induces apoptosis in colorectal cancer cells via mitochondrial autophagy, Food Sci. Hum. Wellness 9 (2020) 237-244. https://doi.org/10.1016/j.fshw.2020.05.001.

[57] H. Liu, L. Zhang, X. Zhang, et al., PI3K/AKT/mTOR pathway promotes progestin resistance in endometrial cancer cells by inhibition of autophagy, Onco Targets Ther. 10 (2017) 2865-2871. https://doi.org/10.2147/OTT.S95267.

[58] D.R. Green, G. Kroemer, Cytoplasmic functions of the tumour suppressor p53, Nature 458 (2009) 1127-1130. https://doi.org/10.1038/nature07986.

[59] M.T. Rosenfeldt, J. O'Prey, J.P. Morton, et al., p53 status determines the role of autophagy in pancreatic tumour development, Nature 504 (2013) 296-300. https://doi.org/10.1038/nature12865.

[60] Y. Qian, C. Shi, C. Cheng, et al., Ginger polysaccharide UGP1 suppressed human colon cancer growth via p53, Bax/Bcl-2, caspase-3 pathways and immunomodulation, Food Sci. Hum. Wellness 12 (2023) 467-476. https://doi.org/10.1016/j.fshw.2022.07.048.

[61] J.A. Pan, Y. Tang, J.Y. Yu, et al., miR-146a attenuates apoptosis and modulates autophagy by targeting TAF9b/P53 pathway in doxorubicin-induced cardiotoxicity, Cell Death Dis. 10 (2019) 668. https://doi.org/10.1038/s41419-019-1901-x.

[62] R. Johnson, S. Shabalala, J. Louw, et al., Aspalathin reverts doxorubicin-induced cardiotoxicity through increased autophagy and decreased expression of p53/mTOR/p62 signaling, Molecules 22 (2017) 1589. https://doi.org/10.3390/molecules22101589.

[63] T. Yu, F. Guo, Y. Yu, et al., *Fusobacterium nucleatum* promotes chemoresistance to colorectal cancer by modulating autophagy, Cell 170 (2017) 548-563. https://doi.org/10.1016/j.cell.2017.07.008.

[64] Y.C. Song, C.C. Kuo, C.T. Liu, et al., Combined effects of Tanshinone IIA and an autophagy inhibitor on the apoptosis of leukemia cells via p53, apoptosis-related proteins and oxidative stress pathways, Integr Cancer Ther. 21 (2022) 15347354221117776. https://doi.org/10.1177/15347354221117776.